*The Canadian Mineralogist*
Vol. 34, pp. 577-593 (1996)

# SODIUM AT THE *A* SITE IN CLINOAMPHIBOLES: THE EFFECTS OF COMPOSITION ON PATTERNS OF ORDER

FRANK C. HAWTHORNE[1], ROBERTA OBERTI AND NICOLA SARDONE

*CNR – Centro di Studio per la Cristallochimica e la Cristallografia, via Abbiategrasso 209, I-27100 Pavia, Italy*

## ABSTRACT

The crystal structures of 12 amphiboles with Na at the *A* site have been refined to *R* indices of ~1.5% using single-crystal Mo*K*α X-ray data. Site populations were assigned from the refined site-scattering values and results of electron-microprobe analysis. Of primary interest is the variation in ordering of Na at the *A* site as a function of composition and site populations in the rest of the structure. High-resolution data were collected with Ag radiation for one crystal, but the results were not materially different from refinements with normal-resolution data collected with Mo radiation. High correlations among parameters and convergence at false minima prevented derivation of reliable partitioning of the *A*-site cations between the *A*(*m*) and *A*(2) sites; thus, the character of the electron density in the *A* cavity was examined with difference-Fourier maps calculated with the *A* cations omitted from the structural model. The variation in electron-density distribution at the *A* site can be rationalized in terms of a number of preferred short-range-ordered configurations involving Na or Ca at the *M*(4) site, OH or F at the O(3) site, and Na at the *A*(*m*) or *A*(2) sites. The relevant arrangements and their relative stability are $^{M(4)}Na\text{–}^{O(3)}F\text{–}^{A(m)}Na$ > $^{M(4)}Ca\text{–}^{O(3)}OH\text{–}^{A(2)}Na$ > $^{M(4)}Na\text{–}^{O(3)}OH\text{–}^{A(m)}Na$ >> $^{M(4)}Ca\text{–}^{O(3)}F\text{–}^{A(m)}Na$ = $^{M(4)}Ca\text{–}^{O(3)}F\text{–}^{A(2)}Na$; this sequence can be understood in terms of local bond-valence requirements within the amphibole structure.

*Keywords:* structure refinement, electron density, amphibole, short-range order, Na ordering.

## SOMMAIRE

La structure cristalline de douze échantillons d'amphibole dans lesquels le Na occupe le site *A* a été affinée jusqu'à un résidu *R* d'environ 1.5% en utilisant des données de diffraction X obtenues sur cristal unique avec un rayonnement Mo*K*α. L'occupation des sites a été déterminée par affinement du pouvoir de dispersion des rayons X selon les divers sites, en tenant compte des compositions déterminées avec une microsonde électronique. Nous nous attardons surtout à la variation dans le degré d'ordre du Na au site *A* en fonction de la composition de l'amphibole et de l'occupation des autres sites de la structure. Nous avons prélevé des données à résolution plus élevée avec un rayonnement Ag dans le cas d'un cristal, mais les résultats ne diffèrent pas vraiment de ceux des affinements effectués sur données prélevées avec rayonnement Mo. Les corrélations élevées parmi les paramètres et la convergence à de faux minimums nous empêchent de dériver de l'information fiable sur la répartition des cations occupant le site *A* entre les sites *A*(*m*) et *A*(2). Ainsi, nous avons examiné la distribution de la densité des électrons autour de la cavité *A* au moyen de projections par différence-Fourier en omettant les cations *A* du modèle structural. On explique la distribution des électrons au site *A* en termes d'agencements préférés impliquant le Na ou le Ca au site *M*(4), OH ou F au site O(3), et Na aux sites *A*(*m*) ou *A*(2). Nous en déduisons les agencements et l'ordre relatif de stabilité suivants: $^{M(4)}Na\text{–}^{O(3)}F\text{–}^{A(m)}Na$ > $^{M(4)}Ca\text{–}^{O(3)}OH\text{–}^{A(2)}Na$ > $^{M(4)}Na\text{–}^{O(3)}OH\text{–}^{A(m)}Na$ >> $^{M(4)}Ca\text{–}^{O(3)}F\text{–}^{A(m)}Na$ = $^{M(4)}Ca\text{–}^{O(3)}F\text{–}^{A(2)}Na$. Cette séquence résulte des exigeances locales en valences de liaison dans la structure d'une amphibole.

(Traduit par la Rédaction)

*Mots-clés:* affinement structural, densité des électrons, amphibole, mise en ordre locale, degré d'ordre du Na.

## INTRODUCTION

In the monoclinic *C*2/*m* amphibole structure, the *A* site is in a large cavity between the back-to-back double chains; it is surrounded by an irregular array of twelve chain-bridging anions (Fig. 1). The site may be unoccupied (as in tremolite) or occupied (as in pargasite), usually by the alkali cations Na and K. Heritsch (1955) first recognized that cation(s) occupying the *A* site could show significant positional disorder. The character of this disorder is most easily expressed in terms of the site nomenclature of Hawthorne & Grundy (1972), as shown in Table 1 and Figure 1. At the center of the cavity, the intersection of

[1] Permanent address: Department of Geological Sciences, University of Manitoba, Winnipeg, Manitoba R3T 2N2.

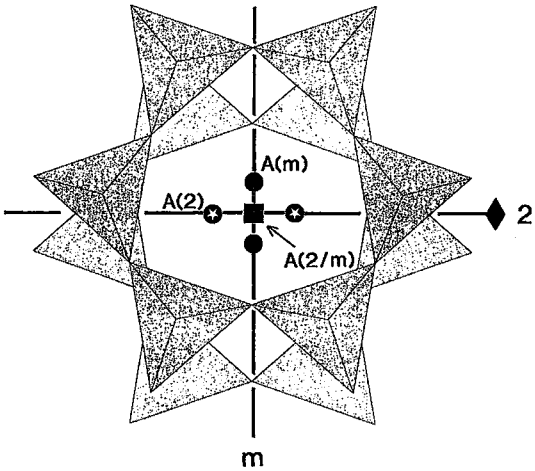


FIG. 1. The *A* cavity and site nomenclature in the *C2/m* amphibole structure; square: *A*(2/*m*); circle: *A*(*m*); starred circle: *A*(2).

a mirror plane and a two-fold axis (Wyckoff symbol 2*b*) is designated the *A*(2/*m*) site; similarly, the other sites [*A*(*m*), *A*(2) and *A*(1)] are designated by their point symmetry. The typical separation between the split and the central positions is in the range 0.4–0.6 Å.

Prewitt (1963) and Gibbs & Prewitt (1968) reported occupancy of the *A*(2) site in synthetic $Na_2H_2Co_5Si_8O_{22}(OH)_2$, and occupancy of the *A*(*m*) site in synthetic $Na_2H_2Mg_5Si_8O_{22}F_2$, leading Gibbs (1966) to suggest that *A*(2) or *A*(*m*) is occupied if O(3) is OH or F, respectively. Papike *et al.* (1969) found strong ordering at the *A*(*m*) site in potassian titanian magnesio-hastingsite and potassium-magnesio-katophorite. Hawthorne & Grundy (1973a, b) showed that both the *A*(2) and *A*(*m*) sites could be occupied in the same crystal. Hawthorne & Grundy (1978) proposed that K is ordered at *A*(*m*) and Na is ordered at *A*(2) in a sample of potassian ferri-taramite. Hawthorne *et al.* (1980) found Na at both the *A*(2) and *A*(*m*) positions in ferroan pargasitic hornblende. Ungaretti *et al.* (1981) showed that K is ordered at the *A*(*m*) site, but that Na can occur at both the *A*(2) and *A*(*m*) sites. Cameron *et al.* (1983) showed that K is ordered completely at *A*(*m*) in synthetic $KCaNaMg_5Si_8O_{22}F_2$, and proposed that Na occupies the general *A*(1) position in synthetic $NaCaNaMg_5Si_8O_{22}F_2$. More recently, Boschmann *et al.* (1994) showed Na to be disordered over the *A*(2) and *A*(*m*) sites in a synthetic fluor-edenite of intermediate composition.

Thus it seems well established that K is ordered at the *A*(*m*) site, and that Na may occur at the *A*(*m*) and *A*(2) sites. However, the factors that affect the ordering behavior of Na are not yet understood; it is the intention of the current study to resolve this problem.

TABLE 1. *A*-SITE NOMENCLATURE IN *C2/m* AMPHIBOLES*

| Site | Wyckoff symbol | Coordinates |
|---|---|---|
| *A*(2/*m*) | 2*b* | 0, ½, 0 |
| *A*(*m*) | 4*i* | *x*, ½, *z* |
| *A*(2) | 4*g* | 0, *y*, 0 |
| *A*(1) | 8*j* | *x*, *y*, *z* |

* After Hawthorne & Grundy (1972)

## EXPERIMENTAL

A set of low-potassium amphiboles [K < 0.05 *apfu* (atoms per formula unit), except for one sample, A(9), in which K = 0.17 *apfu*] was used so as to minimize the problem of differentiating between K and Na at the different *A*-sites. Amphiboles were selected such that the *A* site has high occupancy (>80%) and the overall compositions span as great a range as possible, so as to examine all crystal-chemical factors that could possibly affect the ordering of Na in the *A* cavity. The sample numbers and names are given in Table 2.

### *Collection and refinement of X-ray data*

Unit-cell dimensions were measured and X-ray intensity data were collected and processed according

TABLE 2. SAMPLE NUMBERS AND AMPHIBOLE TYPES FOR THE CRYSTALS USED IN THIS WORK

| | Sample number | SEQ* | Amphibole type |
|---|---|---|---|
| A(1) | DJ102 N.3 | 516 | Fluor-nyböite |
| A(2) | DJ102 N.4 | 518 | Fluor-nyböite |
| A(3) | Q95 N.32 | 504 | Nyböite |
| A(4) | DJ102 N.12 | 521 | Fluor-taramite |
| A(5) | G230F N.3 | 145 | Taramite |
| A(6) | Q99 N.3 | 421 | Taramite |
| A(7) | D163 N.2 | 291 | Katophorite |
| A(8) | D167 N.1 | 242 | Katophorite |
| A(9) | BM47 N.1 | 457 | Pargasite |
| A(10) | FE129 N.1 | 212 | Pargasite |
| A(11) | FE229 N.18 | 328 | Pargasite |
| A(12) | KP N.1 | 505 | Pargasite |

* SEQ = sequence number in Pavia amphibole data-base

TABLE 3. UNIT-CELL DIMENSIONS* AND MISCELLANEOUS DATA CONCERNING STRUCTURE REFINEMENT

| | A(1) | A(2) | A(3) | A(4) | A(5) | A(6) |
|---|---|---|---|---|---|---|
| *a* (Å) | 9.668 | 9.673 | 9.678 | 9.722 | 9.772 | 9.780 |
| *b* (Å) | 17.801 | 17.817 | 17.772 | 17.862 | 17.853 | 17.899 |
| *c* (Å) | 5.309 | 5.315 | 5.310 | 5.319 | 5.310 | 5.319 |
| β (°) | 104.09 | 104.08 | 104.21 | 104.33 | 104.83 | 104.9 |
| *V* (Å³) | 886.2 | 888.6 | 885.4 | 894.8 | 895.6 | 900.8 |
| sin θ/λ (Å⁻¹) | 0.70 | 0.70 | 0.70 | 0.70 | 0.70 | 0.99 |
| # $F_{all}$ | 1348 | 1348 | 1346 | 1355 | 1350 | 1375 |
| # $F_{obs}$ | 949 | 994 | 962 | 899 | 1003 | 1082 |
| $R_{symm}$ | 1.3 | 1.2 | 1.5 | 1.7 | 1.4 | 1.0 |
| $R_{obs}$ | 1.4 | 1.4 | 1.4 | 1.5 | 1.4 | 1.2 |
| $R_{all}$ | 2.6 | 2.5 | 2.6 | 3.2 | 2.4 | 2.1 |
| | A(7) | A(8) | A(9) | A(10) | A(11) | A(12) |
| *a* (Å) | 9.737 | 9.775 | 9.870 | 9.839 | 9.854 | 9.862 |
| *b* (Å) | 17.875 | 17.928 | 17.991 | 17.963 | 17.931 | 17.928 |
| *c* (Å) | 5.314 | 5.313 | 5.291 | 5.291 | 5.282 | 5.295 |
| β (°) | 104.64 | 104.69 | 105.08 | 105.17 | 105.33 | 105.28 |
| *V* (Å³) | 894.8 | 900.7 | 907.1 | 902.6 | 900.2 | 903.1 |
| sin θ/λ (Å⁻¹) | 0.87 | 0.70 | 0.70 | 1.84 | 1.21 | 0.81 |
| # $F_{all}$ | 810 | 1368 | 1375 | 5488 | 3004 | 1455 |
| # $F_{obs}$ | 808 | 849 | 1122 | 5102 | 2962 | 1128 |
| $R_{symm}$ | 1.4 | 1.8 | 1.0 | 2.1 | 1.2 | 1.3 |
| $R_{obs}$ | 1.2 | 1.5 | 1.5 | 2.6 | 1.6 | 1.4 |
| $R_{all}$ | 1.2 | 3.6 | 2.1 | 2.6 | 1.6 | 2.1 |

* Standard deviations are ≤0.002, <0.004, <0.001 Å, ≤0.01° and ≤0.4 Å³ for *a*, *b*, *c*, β, *V*, respectively.

to the procedures of Oberti *et al.* (1992). Table 3 lists the cell dimensions and information pertinent to data collection and structure refinement.

The crystal structures were initially refined according to the procedures described by Ungaretti (1980), and converged to *R* indices of ~1.5% for an anisotropic displacement model and with the scattering from the *M*(1), *M*(2), *M*(3), *M*(4), *A*(2/*m*), *A*(*m*), and *A*(2) sites considered as variable. A model with all the *A*(2/*m*), *A*(*m*) and *A*(2) sites occupied allows a better fit to be obtained for the aggregate electron-density in the *A* cavity, and also results in the maximum estimate for the *A*-site scattering. The $F_o$ maps calculated at this stage showed the distribution of electron density in the *A* cavity. This information was used in the subsequent refinements to distribute the *A*-site cations between *A*(*m*) and *A*(2) only. This model seems physically more reasonable, as it takes into account the size and coordination of Na and K, together with the fact that Na or K at the central *A*(2/*m*) site cannot satisfy their own bond-valence requirements (Hawthorne 1983). Final atomic coordinates and equivalent isotropic-displacement factors are given in Table 4, selected interatomic distances are given in Table 5, and the refined site-scattering values are given in Table 6. Observed and calculated structure-factors and anisotropic displacement parameters may be obtained from the Depository of Unpublished Data, CISTI, National Research Council of Canada, Ottawa, Ontario K1A 0S2.

*Collection and refinement of high-resolution data*

One of the problems associated with characterizing the details of the *A*-site configuration is that we are looking at a feature that is approaching the limits of resolution of X-ray diffraction. Consequently, we decided to examine this aspect of the problem in some detail. Data for crystal A(10) were collected with Ag radiation up to a θ value of 67° ($\sin\theta/\lambda = 1.84$ Å$^{-1}$, resolution ≈ 0.19 Å), resulting in 5102 observed reflections (Table 3). Difference-Fourier maps through the *A*(2/*m*) site were calculated with the *A* cations removed from the model (Fig. 2). Although resolution was definitely improved by using higher-angle data in the difference-Fourier calculations, no new information was gained, and correlation problems in the structure refinement were not significantly improved. As the high-resolution data did not lead to any significant improvement in the details of refinement over our usual procedures ($\sin\theta/\lambda = 0.70$ Å$^{-1}$, resolution ≈ 0.49 Å), the other crystals were treated in the standard manner (Table 3).

*Electron-microprobe analysis*

The crystals used in the collection of the X-ray intensity data were subsequently analyzed by electron microprobe (EMP) according to the procedures of Hawthorne *et al.* (1993); the results are given in Table 7. Unit formulae were calculated on the basis of 24 (O,OH,F) assuming OH + F = 2.0 *apfu*; the $Fe^{3+}$ and $Fe^{2+}$ contents were taken from SREF (structure refinement) site-populations.

## Site Populations

It is important to derive the site populations for these amphiboles, as the details of the site populations are expected to affect the pattern of order of Na over the *A* sites.

*The T sites*

The <*T*(2)–O> distances are in the range 1.628–1.635 Å; as discussed by Oberti *et al.* (1995a), these values are characteristic of complete Si occupancy of *T*(2), the variations in <*T*(2)–O> being the result of inductive effects from the rest of the structure. Thus $^{[4]}$Al is completely ordered at *T*(1), and its estimates from EMP show good agreement with the <*T*(1)–O> *versus* $^{T(1)}$Al relationship of Oberti *et al.* (1995a).

*The M sites*

In the past, it has usually been assumed that the *M*(1) and *M*(3) sites are occupied only by Mg and $Fe^{2+}$ (except in kaersutite). However, evidence is accumu-

TABLE 4. ATOMIC COORDINATES AND EQUIVALENT ISOTROPIC DISPLACEMENT FACTORS ($A^2$)*

| | | A(1) | A(2) | A(3) | A(4) | A(5) | A(6) | A(7) | A(8) | A(9) | A(10) | A(11) | A(12) |
|---|---|---|---|---|---|---|---|---|---|---|---|---|---|
| O(1) | *x* | 0.1077 | 0.1077 | 0.1064 | 0.1069 | 0.1048 | 0.1047 | 0.1054 | 0.1055 | 0.1076 | 0.1064 | 0.1062 | 0.1054 |
| | *y* | 0.0907 | 0.0908 | 0.0916 | 0.0902 | 0.0918 | 0.0920 | 0.0923 | 0.0914 | 0.0869 | 0.0884 | 0.0873 | 0.0888 |
| | *z* | 0.2091 | 0.2091 | 0.2086 | 0.2107 | 0.2115 | 0.2116 | 0.2094 | 0.2111 | 0.2183 | 0.2146 | 0.2148 | 0.2142 |
| | $B_{eq}$ | 0.76 | 0.76 | 0.64 | 0.80 | 0.70 | 0.73 | 0.76 | 0.86 | 0.74 | 0.89 | 0.89 | 0.98 |
| O(2) | *x* | 0.1184 | 0.1185 | 0.1181 | 0.1190 | 0.1192 | 0.1196 | 0.1191 | 0.1201 | 0.1193 | 0.1198 | 0.1197 | 0.1195 |
| | *y* | 0.1716 | 0.1719 | 0.1724 | 0.1724 | 0.1737 | 0.1743 | 0.1743 | 0.1743 | 0.1719 | 0.1740 | 0.1736 | 0.1736 |
| | *z* | 0.7431 | 0.7429 | 0.7446 | 0.7409 | 0.7431 | 0.7426 | 0.7438 | 0.7413 | 0.7297 | 0.7350 | 0.7344 | 0.7365 |
| | $B_{eq}$ | 0.72 | 0.74 | 0.62 | 0.73 | 0.63 | 0.67 | 0.68 | 0.78 | 0.73 | 0.70 | 0.67 | 0.76 |
| O(3) | *x* | 0.1085 | 0.1090 | 0.1096 | 0.1085 | 0.1095 | 0.1096 | 0.1098 | 0.1095 | 0.1074 | 0.1086 | 0.1074 | 0.1080 |
| | *z* | 0.7065 | 0.7063 | 0.7080 | 0.7083 | 0.7093 | 0.7095 | 0.7085 | 0.7102 | 0.7151 | 0.7169 | 0.7195 | 0.7155 |
| | $B_{eq}$ | 0.96 | 0.96 | 0.66 | 0.94 | 0.72 | 0.72 | 0.86 | 0.87 | 0.84 | 0.80 | 0.82 | 0.88 |
| O(4) | *x* | 0.3665 | 0.3667 | 0.3675 | 0.3666 | 0.3685 | 0.3687 | 0.3694 | 0.3692 | 0.3660 | 0.3684 | 0.3677 | 0.3672 |
| | *y* | 0.2526 | 0.2526 | 0.2530 | 0.2522 | 0.2525 | 0.2520 | 0.2520 | 0.2514 | 0.2497 | 0.2505 | 0.2505 | 0.2509 |
| | *z* | 0.8002 | 0.7999 | 0.8003 | 0.7967 | 0.7957 | 0.7945 | 0.7959 | 0.7933 | 0.7871 | 0.7885 | 0.7870 | 0.7900 |
| | $B_{eq}$ | 0.87 | 0.87 | 0.78 | 0.89 | 0.73 | 0.73 | 0.83 | 0.98 | 1.05 | 0.94 | 0.88 | 0.85 |
| O(5) | *x* | 0.3542 | 0.3543 | 0.3546 | 0.3538 | 0.3537 | 0.3535 | 0.3536 | 0.3528 | 0.3493 | 0.3508 | 0.3507 | 0.3510 |
| | *y* | 0.1338 | 0.1340 | 0.1355 | 0.1363 | 0.1398 | 0.1399 | 0.1386 | 0.1391 | 0.1387 | 0.1413 | 0.1419 | 0.1408 |
| | *z* | 0.0936 | 0.0936 | 0.0969 | 0.0977 | 0.1086 | 0.1089 | 0.1053 | 0.1064 | 0.1078 | 0.1137 | 0.1153 | 0.1129 |
| | $B_{eq}$ | 1.03 | 1.06 | 0.99 | 1.11 | 0.87 | 0.88 | 0.97 | 1.01 | 1.04 | 0.90 | 0.85 | 0.91 |
| O(6) | *x* | 0.3426 | 0.3424 | 0.3414 | 0.3430 | 0.3424 | 0.3425 | 0.3423 | 0.3428 | 0.3442 | 0.3435 | 0.3434 | 0.3430 |
| | *y* | 0.1202 | 0.1203 | 0.1196 | 0.1194 | 0.1176 | 0.1178 | 0.1188 | 0.1179 | 0.1155 | 0.1161 | 0.1150 | 0.1159 |
| | *z* | 0.5921 | 0.5925 | 0.5969 | 0.5978 | 0.6095 | 0.6094 | 0.6040 | 0.6054 | 0.6080 | 0.6112 | 0.6148 | 0.6140 |
| | $B_{eq}$ | 0.92 | 0.94 | 0.93 | 0.95 | 0.90 | 0.88 | 0.93 | 1.06 | 1.08 | 1.05 | 1.02 | 1.00 |
| O(7) | *x* | 0.3391 | 0.3392 | 0.3373 | 0.3408 | 0.3382 | 0.3381 | 0.3372 | 0.3386 | 0.3403 | 0.3397 | 0.3413 | 0.3396 |
| | *z* | 0.2910 | 0.2907 | 0.2871 | 0.2862 | 0.2763 | 0.2763 | 0.2801 | 0.2786 | 0.2769 | 0.2714 | 0.2686 | 0.2725 |
| | $B_{eq}$ | 1.11 | 1.17 | 1.13 | 1.13 | 1.08 | 1.08 | 1.14 | 1.26 | 1.21 | 1.13 | 1.04 | 1.11 |
| *T*(1) | *x* | 0.2824 | 0.2826 | 0.2820 | 0.2826 | 0.2810 | 0.2809 | 0.2811 | 0.2810 | 0.2808 | 0.2807 | 0.2808 | 0.2800 |
| | *y* | 0.0869 | 0.0869 | 0.0874 | 0.0866 | 0.0870 | 0.0869 | 0.0869 | 0.0865 | 0.0854 | 0.0855 | 0.0854 | 0.0859 |
| | *z* | 0.2966 | 0.2966 | 0.2980 | 0.2983 | 0.3022 | 0.3021 | 0.3004 | 0.3007 | 0.3017 | 0.3023 | 0.3031 | 0.3032 |
| | $B_{eq}$ | 0.48 | 0.50 | 0.44 | 0.50 | 0.43 | 0.44 | 0.44 | 0.48 | 0.46 | 0.43 | 0.43 | 0.49 |
| *T*(2) | *x* | 0.2916 | 0.2917 | 0.2917 | 0.2919 | 0.2920 | 0.2921 | 0.2924 | 0.2923 | 0.2902 | 0.2914 | 0.2911 | 0.2907 |
| | *y* | 0.1732 | 0.1732 | 0.1737 | 0.1732 | 0.1741 | 0.1740 | 0.1738 | 0.1736 | 0.1725 | 0.1733 | 0.1734 | 0.1737 |
| | *z* | 0.8093 | 0.8094 | 0.8115 | 0.8108 | 0.8157 | 0.8157 | 0.8141 | 0.8134 | 0.8096 | 0.8135 | 0.8139 | 0.8147 |
| | $B_{eq}$ | 0.52 | 0.52 | 0.46 | 0.52 | 0.41 | 0.43 | 0.46 | 0.52 | 0.52 | 0.49 | 0.46 | 0.49 |
| *M*(1) | *y* | 0.0906 | 0.0908 | 0.0904 | 0.0906 | 0.0899 | 0.0901 | 0.0903 | 0.0903 | 0.0876 | 0.0894 | 0.0894 | 0.0900 |
| | $B_{eq}$ | 0.57 | 0.58 | 0.54 | 0.59 | 0.54 | 0.55 | 0.56 | 0.61 | 0.68 | 0.53 | 0.50 | 0.53 |
| *M*(2) | *y* | 0.1796 | 0.1798 | 0.1796 | 0.1792 | 0.1781 | 0.1782 | 0.1784 | 0.1782 | 0.1773 | 0.1764 | 0.1762 | 0.1770 |
| | $B_{eq}$ | 0.59 | 0.57 | 0.52 | 0.61 | 0.54 | 0.54 | 0.55 | 0.56 | 0.57 | 0.50 | 0.47 | 0.50 |
| *M*(3) | $B_{eq}$ | 0.62 | 0.59 | 0.56 | 0.60 | 0.49 | 0.49 | 0.53 | 0.52 | 0.56 | 0.51 | 0.46 | 0.49 |
| *M*(4) | *y* | 0.2778 | 0.2781 | 0.2786 | 0.2789 | 0.2804 | 0.2806 | 0.2797 | 0.2793 | 0.2784 | 0.2803 | 0.2801 | 0.2803 |
| | $B_{eq}$ | 0.95 | 0.97 | 0.98 | 1.00 | 0.75 | 0.77 | 0.77 | 0.88 | 0.83 | 0.65 | 0.61 | 0.72 |
| *M*(4′) | *y* | – | – | – | – | – | – | 0.2568 | 0.2535 | 0.2532 | 0.2599 | 0.2594 | – |
| | $B_{eq}$ | – | – | – | – | – | – | 2.08 | 1.03 | 1.08 | 0.80 | 0.74 | – |
| *A*(*m*) | *x* | 0.0546 | 0.0552 | 0.0492 | 0.0521 | 0.0304 | 0.0369 | 0.0437 | 0.0444 | 0.0326 | 0.0221 | 0.0168 | 0.0100 |
| | *z* | 0.1162 | 0.1186 | 0.1126 | 0.1144 | 0.0806 | 0.0896 | 0.1004 | 0.0978 | 0.0697 | 0.0585 | 0.0413 | 0.0191 |
| | $B_{eq}$ | 3.06 | 2.88 | 2.82 | 3.01 | 3.13 | 2.92 | 3.43 | 3.10 | 3.45 | 2.54 | 4.37 | 4.16 |
| *A*(2) | *y* | 0.4836 | 0.4829 | 0.4789 | 0.4797 | 0.4735 | 0.4733 | 0.4747 | 0.4742 | 0.4758 | 0.4730 | 0.4703 | 0.4706 |
| | $B_{eq}$ | 5.64 | 5.20 | 3.59 | 4.30 | 2.48 | 2.87 | 2.95 | 3.40 | 3.40 | 2.65 | 2.09 | 2.42 |
| H | *x* | 0.1854 | 0.2031 | 0.1984 | 0.1932 | 0.1981 | 0.1960 | 0.1880 | 0.1792 | 0.1860 | 0.1922 | 0.1900 | 0.2102 |
| | *z* | 0.7444 | 0.7650 | 0.7513 | 0.7615 | 0.7682 | 0.7625 | 0.7562 | 0.7448 | 0.7687 | 0.7658 | 0.7689 | 0.7705 |
| | $B_{eq}$ | 7.93 | 1.22 | 2.35 | 2.25 | 1.34 | 1.71 | 1.15 | 0.85 | 0.79 | 0.50 | 1.79 | 5.80 |

O(3) = *x*,0,*z*; O(7) = *x*,0,*z*; *M*(1) = 0,*y*,½; *M*(2) = 0,*y*,0; *M*(3) = 0,0,0; *M*(4) = 0,*y*,½; *M*(4′) = 0,*y*,½; *A*(*m*) = *x*,½,*z*; *A*(2) = 0,*y*,0; H = *y*,0,*z*.
* Standard deviations are ≤1 in the final digit, except for *A*(*m*) and *A*(2), which are <5 in the final digit.

TABLE 5. SELECTED INTERATOMIC DISTANCES (Å)

| | | A(1) | A(2) | A(3) | A(4) | A(5) | A(6) | A(7) | A(8) | A(9) | A(10) | A(11) | A(12) |
|---|---|---|---|---|---|---|---|---|---|---|---|---|---|
| *T*(1)–O(1) | | 1.641 | 1.643 | 1.650 | 1.657 | 1.668 | 1.669 | 1.659 | 1.663 | 1.651 | 1.656 | 1.660 | 1.662 |
| *T*(1)–O(5) | | 1.644 | 1.647 | 1.653 | 1.664 | 1.680 | 1.684 | 1.673 | 1.677 | 1.671 | 1.685 | 1.687 | 1.687 |
| *T*(1)–O(6) | | 1.645 | 1.649 | 1.652 | 1.662 | 1.679 | 1.684 | 1.672 | 1.675 | 1.668 | 1.682 | 1.684 | 1.686 |
| *T*(1)–O(7) | | 1.644 | 1.645 | 1.648 | 1.654 | 1.669 | 1.670 | 1.659 | 1.664 | 1.661 | 1.664 | 1.670 | 1.671 |
| <*T*(1)–O> | | 1.644 | 1.646 | 1.651 | 1.659 | 1.674 | 1.677 | 1.666 | 1.670 | 1.663 | 1.672 | 1.675 | 1.676 |
| *T*(2)–O(2) | | 1.626 | 1.626 | 1.630 | 1.630 | 1.633 | 1.633 | 1.633 | 1.629 | 1.628 | 1.629 | 1.629 | 1.629 |
| *T*(2)–O(4) | | 1.594 | 1.597 | 1.597 | 1.598 | 1.604 | 1.604 | 1.601 | 1.601 | 1.595 | 1.603 | 1.600 | 1.598 |
| *T*(2)–O(5) | | 1.641 | 1.641 | 1.636 | 1.634 | 1.636 | 1.638 | 1.637 | 1.640 | 1.650 | 1.646 | 1.644 | 1.644 |
| *T*(2)–O(6) | | 1.655 | 1.653 | 1.651 | 1.653 | 1.653 | 1.654 | 1.651 | 1.655 | 1.664 | 1.658 | 1.659 | 1.662 |
| <*T*(2)–O> | | 1.629 | 1.629 | 1.628 | 1.629 | 1.631 | 1.632 | 1.630 | 1.631 | 1.634 | 1.634 | 1.633 | 1.633 |
| *M*(1)–O(1) | x2 | 2.062 | 2.064 | 2.058 | 2.059 | 2.049 | 2.053 | 2.059 | 2.055 | 2.042 | 2.051 | 2.049 | 2.050 |
| *M*(1)–O(2) | x2 | 2.081 | 2.085 | 2.095 | 2.093 | 2.120 | 2.129 | 2.125 | 2.128 | 2.103 | 2.116 | 2.104 | 2.105 |
| *M*(1)–O(3) | x2 | 2.084 | 2.090 | 2.086 | 2.093 | 2.085 | 2.093 | 2.092 | 2.099 | 2.067 | 2.097 | 2.094 | 2.097 |
| <*M*(1)–O> | | 2.076 | 2.080 | 2.080 | 2.081 | 2.082 | 2.092 | 2.092 | 2.094 | 2.071 | 2.088 | 2.083 | 2.084 |
| *M*(2)–O(1) | x2 | 2.064 | 2.066 | 2.044 | 2.070 | 2.024 | 2.026 | 2.021 | 2.039 | 2.113 | 2.064 | 2.073 | 2.059 |
| *M*(2)–O(2) | x2 | 1.988 | 1.990 | 1.981 | 2.010 | 2.010 | 2.018 | 2.001 | 2.022 | 2.078 | 2.055 | 2.058 | 2.051 |
| *M*(2)–O(4) | x2 | 1.892 | 1.892 | 1.880 | 1.912 | 1.910 | 1.920 | 1.908 | 1.930 | 1.993 | 1.974 | 1.980 | 1.964 |
| <*M*(2)–O> | x2 | 1.981 | 1.983 | 1.968 | 1.998 | 1.981 | 1.988 | 1.977 | 1.997 | 2.061 | 2.031 | 2.037 | 2.025 |
| *M*(3)–O(1) | x4 | 2.088 | 2.092 | 2.092 | 2.087 | 2.099 | 2.106 | 2.106 | 2.102 | 2.066 | 2.070 | 2.050 | 2.069 |
| *M*(3)–O(3) | x2 | 2.079 | 2.085 | 2.082 | 2.081 | 2.091 | 2.096 | 2.092 | 2.086 | 2.056 | 2.055 | 2.036 | 2.061 |
| <*M*(3)–O> | | 2.085 | 2.090 | 2.089 | 2.085 | 2.096 | 2.103 | 2.101 | 2.096 | 2.063 | 2.065 | 2.045 | 2.067 |
| *M*(4)–O(2) | x2 | 2.415 | 2.417 | 2.413 | 2.422 | 2.425 | 2.424 | 2.412 | 2.409 | 2.406 | 2.411 | 2.408 | 2.415 |
| *M*(4)–O(4) | x2 | 2.346 | 2.346 | 3.346 | 2.344 | 2.344 | 2.341 | 2.329 | 2.319 | 2.314 | 2.312 | 2.311 | 2.334 |
| *M*(4)–O(5) | x2 | 2.764 | 2.761 | 2.724 | 2.718 | 2.621 | 2.623 | 2.656 | 2.657 | 2.672 | 2.597 | 2.583 | 2.603 |
| *M*(4)–O(6) | x2 | 2.492 | 2.491 | 2.507 | 2.508 | 2.546 | 2.546 | 2.527 | 2.551 | 2.607 | 2.580 | 2.604 | 2.592 |
| *A*(*m*)–O(5) | x2 | 3.053 | 3.061 | 3.045 | 3.092 | 3.060 | 3.098 | 3.096 | 3.126 | 3.119 | 3.103 | 3.106 | 3.081 |
| *A*(*m*)–O(5) | x2 | 2.858 | 2.867 | 2.900 | 2.924 | 3.017 | 3.019 | 2.980 | 2.993 | 3.006 | 3.071 | 3.071 | 3.041 |
| *A*(*m*)–O(6) | x2 | 2.686 | 2.682 | 2.687 | 2.675 | 2.760 | 2.727 | 2.707 | 2.699 | 2.761 | 2.818 | 2.851 | 2.952 |
| *A*(*m*)–O(7) | | 2.478 | 2.477 | 2.449 | 2.446 | 2.368 | 2.402 | 2.434 | 2.439 | 2.426 | 2.355 | 2.352 | 2.411 |
| *A*(*m*)–O(7) | | 2.610 | 2.619 | 2.618 | 2.593 | 2.546 | 2.551 | 2.572 | 2.543 | 2.477 | 2.479 | 2.418 | 2.405 |
| *A*(*m*)–O(7) | | 3.064 | 3.056 | 3.106 | 3.099 | 3.327 | 3.279 | 3.202 | 3.219 | 3.357 | 3.449 | 3.542 | 3.652 |
| *A*(2)–O(5) | x2 | 2.633 | 2.629 | 2.594 | 2.636 | 2.625 | 2.631 | 2.617 | 2.632 | 2.691 | 2.682 | 2.656 | 2.641 |
| *A*(2)–O(6) | x2 | 2.969 | 2.965 | 2.896 | 2.902 | 2.773 | 2.776 | 2.819 | 2.801 | 2.778 | 2.740 | 2.683 | 2.705 |
| *A*(2)–O(7) | x2 | 2.467 | 2.464 | 2.475 | 2.452 | 2.462 | 2.469 | 2.475 | 2.465 | 2.453 | 2.443 | 2.432 | 2.462 |
| O(5)–O(6)–O(5) | | 168.6 | 168.5 | 166.8 | 166.4 | 162.5 | 162.6 | 164.2 | 163.3 | 162.0 | 160.4 | 159.1 | 160.6 |

Standard deviations are ~1 in the final digit, except for *A*(*m*)-O and *A*(2)-O, which are <0.007.

lating that the situation is more complicated than this. In non-kaersutitic amphiboles, small amounts of $Ti^{4+}$, associated with the presence of $O^{2-}$ at the adjacent O(3) sites (Oberti *et al.* 1992), can occur at the *M*(1) site. In pargasite and pargasitic hornblende, large amounts of Al can occur at the *M*(3) site (Oberti *et al.* 1995b), as can smaller amounts of $Fe^{3+}$ (Bocchio *et al.* 1978, Hawthorne 1983). Thus the assignment of site populations is not straightforward. Figure 3 shows the relations between the <*M*–O> distances and the refined scattering value at that site. For Mg–$Fe^{2+}$ occupancy, simple linear relations are expected; the latter are shown as full lines in Figures 3a and 3b. For the *M*(1) site, the large deviation for crystal A(9) is indicative of a significant $Ti^{4+}$ content at *M*(1); this is also indicated by the short *M*(1)–O(3) distance [*M*(1)–O(3) is less than <*M*(1)–O>] that is characteristic of this substitution (Oberti *et al.* 1992). Crystals A(1), A(2) and A(4) fall significantly below the ideal curve for Mg–$Fe^{2+}$ occupancy, but this is due to their high F-content

TABLE 6. REFINED SITE-SCATTERING VALUES (*epfu*) AT SELECTED CATION AND ANION SITES

| | N* | A(1) | A(2) | A(3) | A(4) | A(5) | A(6) |
|---|---|---|---|---|---|---|---|
| *M*(1) | 2 | 29.17 | 30.50 | 26.43 | 30.88 | 27.34 | 30.54 |
| *M*(2) | 2 | 32.65 | 34.20 | 33.07 | 36.79 | 33.66 | 34.14 |
| *M*(3) | 1 | 15.45 | 16.45 | 14.77 | 16.96 | 15.52 | 18.24 |
| *M*(4) | 2 | 25.94 | 26.10 | 25.90 | 29.45 | 32.30 | 33.78 |
| O(3) | 2 | 17.24 | 17.20 | 16.60 | 17.24 | 16.00 | 16.00 |
| *A*(*m*) | 2 | 5.84 | 5.80 | 3.26 | 6.06 | 2.34 | 2.64 |
| *A*(2) | 2 | 3.98 | 4.04 | 6.34 | 4.46 | 8.42 | 8.30 |
| | N* | A(7) | A(8) | A(9) | A(10) | A(11) | A(12) |
| *M*(1) | 2 | 31.49 | 32.86 | 28.86 | 27.52 | 26.12 | 28.40 |
| *M*(2) | 2 | 30.28 | 31.61 | 29.20 | 27.89 | 26.26 | 27.25 |
| *M*(3) | 1 | 18.67 | 18.73 | 14.47 | 14.37 | 13.48 | 15.55 |
| *M*(4) | 2 | 33.71 | 35.68 | 36.83 | 40.82 | 39.90 | 37.57 |
| O(3) | 2 | 16.44 | 16.42 | 16.00 | 16.00 | 16.24 | 16.00 |
| *A*(*m*) | 2 | 4.00 | 4.16 | 5.00 | 1.58 | 3.82 | 2.92 |
| *A*(2) | 2 | 5.66 | 6.14 | 6.88 | 7.18 | 6.28 | 8.38 |

* N = number of sites in the structural formula.

(Table 7); correction for the F content of O(3) brings all the crystals [except A(9)] colinear with the ideal Mg–$Fe^{2+}$ line, indicating that their site populations can be assigned directly from the refined site-scattering values (Table 6). For the *M*(3) site, the amphiboles fall into two groups. All crystals of pargasite lie well below the ideal Mg–$Fe^{2+}$ substitution line, the result of the incorporation of Al at *M*(3), as shown by Oberti *et al.* (1995b). The other amphiboles are approximately colinear with the ideal relation if allowance is made for their F content; thus their site populations were calculated as Mg and $Fe^{2+}$ from the refined site-scattering values. The $^{M(3)}$Al contents of the pargasite crystals were derived as discussed by Oberti *et al.* (1995b).

The *M*(2) site is normally occupied by Mg, $Fe^{2+}$, Al and $Fe^{3+}$, with (usually) minor amounts of $Ti^{4+}$ and $Cr^{3+}$ also assigned to this site. Hence, all trivalent and tetravalent *C*-group cations (except $^{M(1)}Ti^{4+}$ and $^{M(3)}$Al) were assigned to *M*(2), and the balance of the scattering was calculated as Mg and $Fe^{2+}$.

The *M*(4) site is occupied by Ca, Na, $Mn^{2+}$, $Fe^{2+}$ and Mg. All Ca calculated from the EMP analysis was assigned to *M*(4), together with any "excess" $Mn^{2+}$ and $Fe^{2+}$ from the *C*-group cations; the remainder of the site was filled with Na. Final site-populations are given in Table 8.

### *Agreement between SREF and EMP data*

The agreement between the total effective scattering by the two methods is shown in Figure 4. There is excellent agreement between the two sets of values, with a mean absolute deviation of 0.81 *e* (~0.7%). Agreement for the individual groups is as follows: *A* = 0.21 *e* (2.0%); *B* = 0.33 *e* (1.0%); *C* = 0.67 *e* (0.9%).

## Cation Disorder at the *A* Site: Experimental Results

### *Difference-Fourier maps*

The electron density in the *A* cavity has always been shown in Fourier or difference-Fourier maps parallel to (010) and (100) (Papike *et al.* 1969, Hawthorne & Grundy 1972); such sections are shown for crystal A(3) in Figures 5a and 5b. It is somewhat difficult to

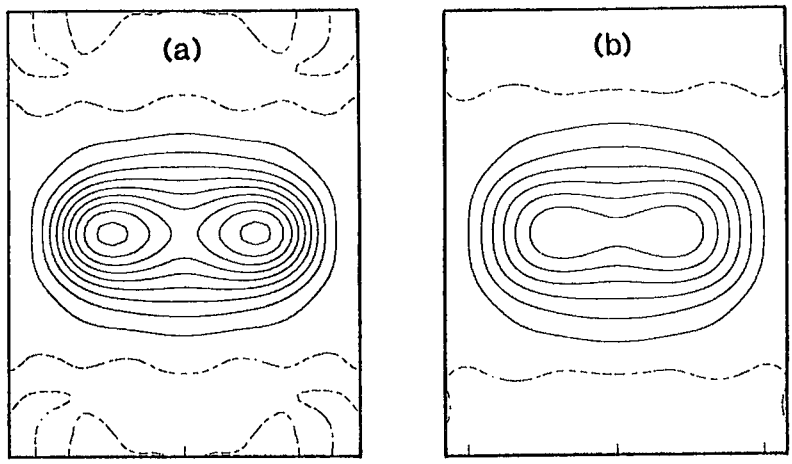


FIG. 2. Comparison of difference-Fourier maps in the vicinity of the *A* site for crystal A(10), projected onto ($\bar{2}$01): (a) calculated with high-angle data ($\sin\theta/\lambda \leq 1.84$ Å$^{-1}$); (b) calculated with standard data ($\sin\theta/\lambda \leq 0.70$ Å$^{-1}$).

TABLE 7. RESULTS (wt%) OF ELECTRON-MICROPROBE ANALYSIS AND CHEMICAL FORMULAE OF THE CRYSTALS USED IN THE STRUCTURE REFINEMENT

| | A(1) | A(2) | A(3) | A(4) | A(5) | A(6) | A(7) | A(8) | A(9) | A(10) | A(11) | A(12) |
|---|---|---|---|---|---|---|---|---|---|---|---|---|
| $SiO_2$ | 50.40 | 49.09 | 48.87 | 44.96 | 44.09 | 42.00 | 44.34 | 41.98 | 44.58 | 43.28 | 42.99 | 42.50 |
| $Al_2O_3$ | 12.35 | 12.27 | 14.86 | 13.07 | 17.28 | 18.20 | 16.15 | 15.34 | 11.29 | 16.47 | 16.96 | 17.41 |
| $TiO_2$ | 0.13 | 0.12 | 0.29 | 0.15 | 0.38 | 0.31 | 0.35 | 0.26 | 0.98 | 0.17 | 0.12 | 0.04 |
| $Cr_2O_3$ | 0.03 | 0.05 | 0.02 | 0.06 | – | – | 0.03 | 0.02 | 2.40 | – | 0.28 | 0.05 |
| $Fe_2O_3$ | 2.44 | 4.29 | 3.57 | 7.58 | 4.70 | 3.39 | 2.17 | 2.50 | 0.80 | 0.66 | 0.19 | 0.31 |
| FeO | 6.98 | 7.99 | 4.23 | 6.77 | 3.47 | 8.74 | 9.48 | 11.84 | 4.48 | 6.38 | 3.46 | 5.36 |
| MnO | 0.07 | 0.10 | 0.01 | 0.15 | – | – | 0.03 | 0.07 | 0.07 | 0.01 | 0.05 | 0.10 |
| MgO | 12.30 | 11.26 | 13.16 | 11.10 | 13.89 | 11.10 | 11.12 | 10.60 | 17.57 | 16.16 | 17.81 | 15.07 |
| CaO | 3.17 | 3.07 | 2.65 | 5.05 | 7.01 | 7.78 | 7.18 | 7.77 | 9.50 | 11.58 | 11.66 | 11.37 |
| $Na_2O$ | 8.34 | 8.52 | 8.29 | 7.43 | 7.06 | 6.42 | 5.60 | 5.00 | 3.97 | 3.04 | 3.41 | 4.31 |
| $K_2O$ | 0.19 | 0.14 | 0.24 | 0.02 | – | – | 0.12 | 0.19 | 0.95 | 0.10 | 0.06 | 0.21 |
| F | 2.52 | 2.54 | 0.51 | 2.20 | 0.01 | – | 0.55 | 0.74 | 0.15 | – | 0.07 | 0.07 |
| $H_2O$ | (0.91) | (0.88) | (1.88) | (1.00) | (2.12) | (2.06) | (1.80) | (1.65) | (1.99) | (2.12) | (2.08) | (2.05) |
| O=F | −1.06 | −1.07 | −0.21 | −0.93 | −0.01 | – | −0.23 | −0.31 | −0.06 | – | −0.03 | −0.03 |
| Total | 98.77 | 99.25 | 98.37 | 98.61 | 99.99 | 100.00 | 98.69 | 97.65 | 98.67 | 99.97 | 99.11 | 98.82 |
| Chemical formulae (*apfu*): | | | | | | | | | | | | |
| Si | 7.178 | 7.049 | 6.908 | 6.592 | 6.238 | 6.090 | 6.454 | 6.295 | 6.447 | 6.187 | 6.103 | 6.118 |
| Al | 0.822 | 0.951 | 1.092 | 1.408 | 1.762 | 1.910 | 1.546 | 1.705 | 1.553 | 1.813 | 1.897 | 1.882 |
| Sum T | 8.000 | 8.000 | 8.000 | 8.000 | 8.000 | 8.000 | 8.000 | 8.000 | 8.000 | 8.000 | 8.000 | 8.000 |
| Al | 1.251 | 1.126 | 1.384 | 0.851 | 1.120 | 1.200 | 1.225 | 1.006 | 0.371 | 0.937 | 0.941 | 1.072 |
| Ti | 0.014 | 0.013 | 0.031 | 0.017 | 0.040 | 0.034 | 0.038 | 0.029 | 0.106 | 0.018 | 0.013 | 0.004 |
| Cr | 0.003 | 0.006 | 0.002 | 0.007 | – | – | 0.003 | 0.002 | 0.274 | – | 0.031 | 0.006 |
| $Fe^{3+}$ | 0.262 | 0.464 | 0.380 | 0.836 | 0.500 | 0.370 | 0.238 | 0.282 | 0.087 | 0.070 | 0.020 | 0.034 |
| *$Fe^{2+}$ | 0.836 | 0.963 | 0.502 | 0.832 | 0.411 | 1.060 | 1.159 | 1.485 | 0.540 | 0.756 | 0.411 | 0.645 |
| Mn | 0.008 | 0.012 | 0.001 | 0.019 | – | – | 0.004 | 0.009 | 0.009 | 0.001 | 0.006 | 0.012 |
| Mg | 2.612 | 2.410 | 2.773 | 2.426 | 2.929 | 2.400 | 2.413 | 2.370 | 3.788 | 3.413 | 3.770 | 3.234 |
| Sum C | 4.986 | 4.994 | 5.073 | 4.988 | 5.000 | 5.064 | 5.080 | 5.183 | 5.175 | 5.195 | 5.192 | 5.007 |
| Fe, Mn | 0.000 | 0.000 | 0.073 | 0.000 | – | 0.064 | 0.080 | 0.183 | 0.175 | 0.195 | 0.192 | 0.007 |
| Ca | 0.484 | 0.472 | 0.401 | 0.793 | 1.062 | 1.208 | 1.120 | 1.248 | 1.472 | 1.760 | 1.774 | 1.754 |
| Na | 1.516 | 1.528 | 1.526 | 1.207 | 0.938 | 0.728 | 0.800 | 0.569 | 0.353 | 0.045 | 0.034 | 0.239 |
| Sum B | 2.000 | 2.000 | 2.000 | 2.000 | 2.000 | 2.000 | 2.000 | 2.000 | 2.000 | 2.000 | 2.000 | 2.000 |
| Na | 0.787 | 0.844 | 0.746 | 0.905 | 1.000 | 1.078 | 0.780 | 0.885 | 0.759 | 0.791 | 0.905 | 0.964 |
| K | 0.035 | 0.026 | 0.043 | 0.004 | – | – | 0.022 | 0.036 | 0.175 | 0.018 | 0.011 | 0.039 |
| Sum A | 0.822 | 0.870 | 0.789 | 0.909 | 1.000 | 1.078 | 0.802 | 0.921 | 0.934 | 0.809 | 0.916 | 1.003 |
| F | 1.135 | 1.153 | 0.228 | 1.020 | 0.004 | – | 0.253 | 0.351 | 0.068 | – | 0.031 | 0.032 |
| OH | (0.865) | (0.847) | (1.772) | (0.980) | (1.996) | (2.000) | (1.747) | (1.649) | (1.932) | (2.000) | (1.969) | (1.968) |

Values in parentheses have been calculated as described in the text.
* includes minor (<0.01) Ni and Zn.

interpret the relative distribution of electron density from these two sections. As the *A*(*m*), *A*(2/*m*) and *A*(2) sites obey the 2/*m* point-symmetry of the *A* cavity, these sites are all coplanar, and lie very close to the plane ($\bar{2}01$) through the central *A*(2/*m*) site. Thus a Fourier or difference-Fourier map parallel to ($\bar{2}01$) best shows the distribution of electron-density within the *A* cavity; Figure 5c shows such a section for crystal A(3).

A representative series of difference-Fourier maps for the crystals of this study is shown in Figure 6; the different types of difference-Fourier map [types (a)–(e)] exhibited by the crystals of this study are indicated by the letter in the top left-hand corner of each map in Figure 6. In type (a) [crystals A(1), A(2) and A(4)], there are two maxima at the *A*(*m*) position and a saddle point at the *A*(2/*m*) position; in addition, there is a slight distension of the lowest contour along the 2-fold axis. This indicates that Na occurs predominantly at the *A*(*m*) site in these crystals. In crystal A(9) [type (b)], there is a single maximum at the *A*(2/*m*) position, and the contours show equal density along the 2-fold axis and in the mirror plane. This indicates that the *A*(*m*) and *A*(2) sites are equally occupied in crystal A(9). In type-(c) crystals [A(3), A(7) and A(8)], there is a single maximum at the *A*(2/*m*) position, but there is strong elongation along the 2-fold axis and extension also in the mirror plane.

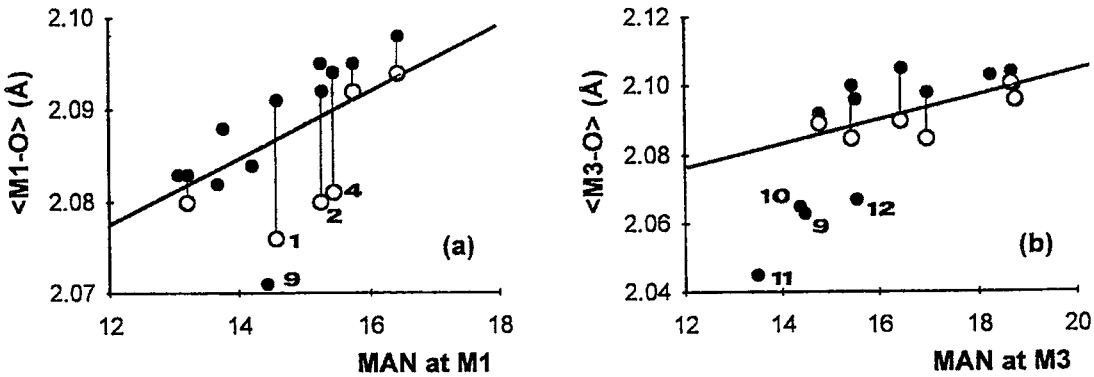


FIG. 3. Variation in <*M*–O> as a function of the mean atomic number (MAN) obtained from SREF for the amphiboles in this study: (a) the *M*(1) site; (b) the *M*(3) site. The lines denote ideal Mg $\rightleftharpoons$ $Fe^{2+}$ substitution according to the curves of Hawthorne (1983); ○ are the observed values, ● are those expected if no $^{O(3)}OH \rightleftharpoons {}^{O(3)}F$ substitution were present.

TABLE 8. SITE POPULATIONS FOR THE *M* SITES

| | | A(1) | A(2) | A(3) | A(4) | A(5) | A(6) |
|---|---|---|---|---|---|---|---|
| *M*(1) | Mg | 1.649 | 1.534 | 1.853 | 1.524 | 1.814 | 1.570 |
| | **$Fe^{2+}$ | 0.351 | 0.466 | 0.147 | 0.476 | 0.186 | 0.430 |
| *M*(2) | Al | 1.255 | 1.127 | 1.384 | 0.853 | 1.120 | 1.200 |
| | Ti | 0.014 | 0.013 | 0.031 | 0.017 | 0.040 | 0.034 |
| | Cr | 0.003 | 0.006 | 0.002 | 0.007 | – | – |
| | $Fe^{3+}$ | 0.263 | 0.465 | 0.380 | 0.838 | 0.500 | 0.370 |
| | $Fe^{2+}$ | 0.258 | 0.193 | 0.172 | 0.031 | – | 0.194 |
| | Mg | 0.207 | 0.196 | 0.031 | 0.254 | 0.340 | 0.202 |
| *M*(3) | Mg | 0.763 | 0.683 | 0.817 | 0.654 | 0.775 | 0.576 |
| | $Fe^{2+}$ | 0.237 | 0.317 | 0.183 | 0.346 | 0.225 | 0.424 |
| | Al | – | – | – | – | – | – |
| *M*(4) | Mn | – | – | 0.001 | – | – | – |
| | $Fe^{2+}$ | – | – | 0.072 | – | – | 0.064 |
| | Ca | 0.484 | 0.472 | 0.401 | 0.793 | 1.062 | 1.208 |
| | Na | 1.516 | 1.528 | 1.526 | 1.207 | 0.938 | 0.728 |
| | | A(7) | A(8) | A(9)* | A(10) | A(11) | A(12) |
| *M*(1) | Mg | 1.493 | 1.366 | 1.635 | 1.748 | 1.848 | 1.685 |
| | **$Fe^{2+}$ | 0.507 | 0.634 | 0.258 | 0.252 | 0.152 | 0.315 |
| *M*(2) | Al | 1.225 | 1.006 | 0.253 | 0.804 | 0.623 | 1.072 |
| | Ti | 0.038 | 0.029 | – | 0.018 | 0.013 | 0.004 |
| | Cr | 0.003 | 0.002 | 0.274 | – | 0.031 | 0.006 |
| | $Fe^{3+}$ | 0.238 | 0.282 | 0.087 | 0.070 | 0.020 | 0.034 |
| | $Fe^{2+}$ | 0.126 | 0.230 | 0.051 | 0.153 | 0.068 | 0.083 |
| | Mg | 0.370 | 0.451 | 1.335 | 0.955 | 1.245 | 0.801 |
| *M*(3) | Mg | 0.541 | 0.519 | 0.714 | 0.710 | 0.609 | 0.747 |
| | $Fe^{2+}$ | 0.459 | 0.481 | 0.168 | 0.157 | 0.073 | 0.253 |
| | Al | – | – | 0.118 | 0.133 | 0.318 | – |
| *M*(4) | Mn | 0.004 | 0.009 | 0.009 | 0.001 | 0.006 | 0.007 |
| | $Fe^{2+}$ | 0.076 | 0.175 | 0.168 | 0.194 | 0.186 | – |
| | Ca | 1.120 | 1.248 | 1.477 | 1.760 | 1.774 | 1.754 |
| | Na | 0.800 | 0.568 | 0.351 | 0.045 | 0.034 | 0.239 |

* *M*(1) includes 0.106 Ti;
** $Fe^{2+}$ includes minor amounts of $Mn^{2+}$ and Ni (<0.01)

In type-(d) crystals [A(5) and A(6)], there are two prominent maxima along the 2-fold axis, a saddle point at *A*(2/*m*), and extension of low contours in the mirror plane. This pattern indicates major occupancy of the *A*(2) position and only minor occupancy of the *A*(*m*) position. In type-(e) crystals [A(10), A(11) and A(12)], there are two prominent maxima along the 2-fold axis, a saddle point at *A*(2/*m*), and no perceptible extension of any contours in the mirror plane; this indicates virtually complete occupancy of the *A*(2) site in this type of crystal.

### *Site-scattering refinement*

The difference-Fourier maps of Figure 6 indicate a wide range of behavior of the electron density within the *A* cavity. This feature also was examined by refinement of the site-scattering at the *A*(*m*) and *A*(2) sites in each crystal. This is quite a sensitive procedure, as the site separations are only marginally larger than the intrinsic resolution of the data, and variable correlation caused problems. Consequently, the difference-Fourier maps of Figure 6 were used as a guide to the starting model and acceptance of the results of the final refinement. Despite these precautions, we are unconvinced that our final results are unique. There were very high correlations among all the variable parameters of the *A* sites. These correlations could be damped by constraining displacement parameters at the *A*(*m*) and *A*(2) sites to be the same, but this resulted in residual density within the cavity. Unconstrained anisotropic refinement of a two-site model could adequately account for all electron density within the *A* cavity; however, the results of specific refinements were not unique, and the displacement values were in many cases not physically realistic. Different starting parameters resulted in slightly

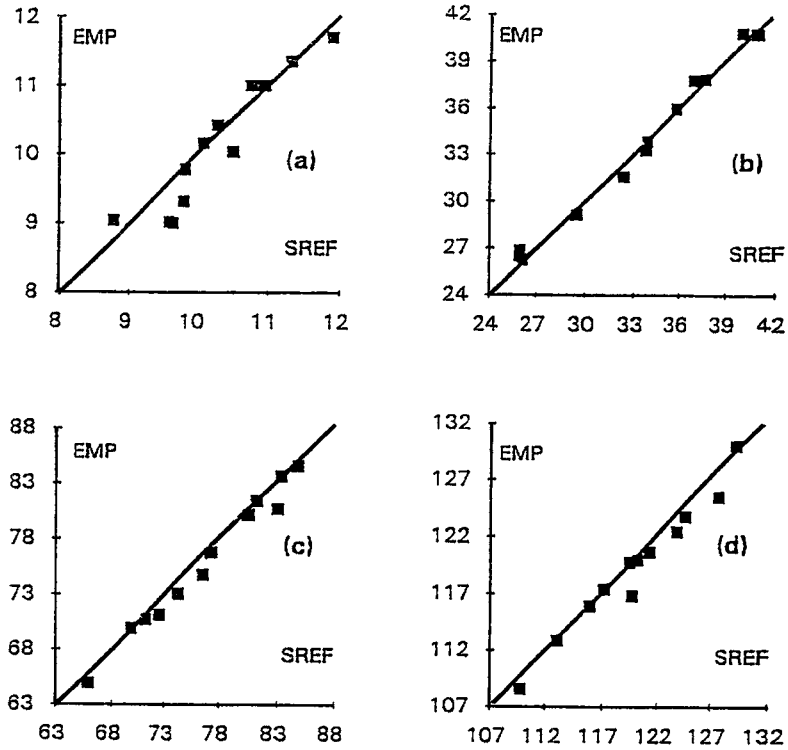


FIG. 4. The total effective scattering (in electrons per formula unit) from the *A*-, *B*-, *C*-group cations (a, b and c, respectively) and from their sum (d) as derived from the unit formulae and as measured by the site-scattering refinement. The lines represent exact agreement between the two measurements.

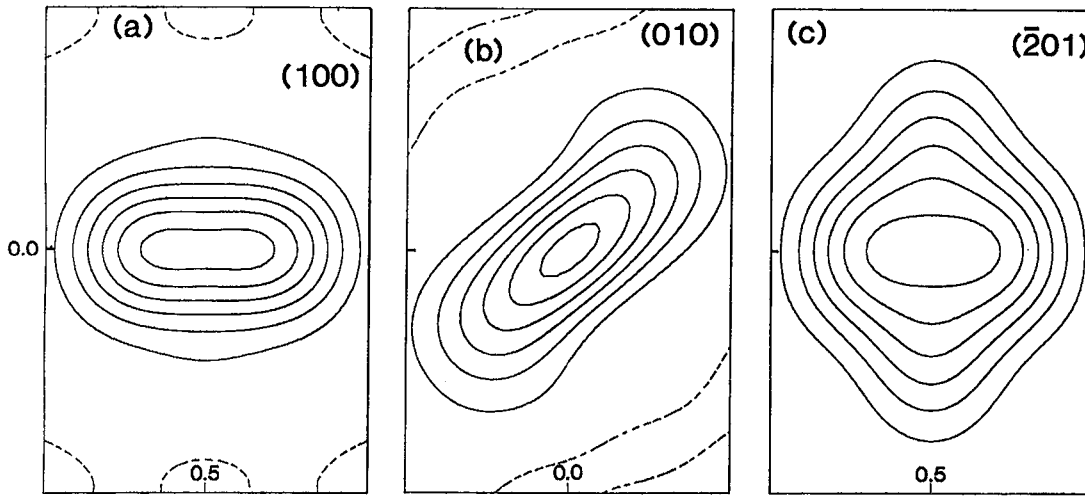


FIG. 5. Difference-Fourier maps (sections) through the *A*(2/*m*) site for crystal A(3), calculated with the *A* cations removed from the structure model: (a) section parallel to (100); (b) section parallel to (010); (c) section parallel to ($\bar{2}$01). The contour interval is 1 *e*/Å$^3$, and the broken line is the zero contour.

different final scattering values at the two sites. However, it should be noted that the *total* scattering from the *A* cations was more or less constant for a given structure, despite the variation at the individual sites. Consequently, we suggest that a visual interpretation of the difference-Fourier maps in Figure 6 provides a better evaluation of the behavior of the cations in the *A* cavity than site-scattering refinement.

## Cation Disorder at the *A* Site: Interpretation

The chemical substitutions that have been suggested as factors affecting the pattern of Na order in the *A* cavity are (1) $^{O(3)}F \rightleftharpoons {}^{O(3)}OH$, (2) $^{B}Na \rightleftharpoons {}^{B}Ca$, (3) $^{C}M^{3+} \rightleftharpoons {}^{C}M^{2+}$ and (4) $^{T}Al \rightleftharpoons {}^{T}Si$; note that substitutions (2), (3) and (4) are not independent in the crystals examined here, as $^{A}Na$ is approximately equal to 1, and hence (2), (3) and (4) are linked by the electroneutrality requirement. However, it is important to recognize that the factors influencing $^{A}Na$ order are short-range rather than long-range, and the presence of SRO (Short-Range Order) may significantly affect the long-range data that we derive from crystal-structure refinement. This situation may be illustrated schematically in Figure 7, in which the O(3) site is occupied by two anions, $X^-$ and $Y^-$. The *A*(2/*m*) site (Fig. 7a) is equally distant from the two closest O(3) sites, whereas the *A*(*m*) site (Fig. 7b) is displaced toward one of the two O(3) sites. Suppose that (1) occupancy of O(3) by $Y^-$ couples to local occupancy of *A*(*m*) by $^{A}Na$, (2) occupancy of O(3) by $X^-$ couples to local occupancy of *A*(2) (not shown) by $^{A}Na$, and (3) arrangement (1) is energetically much more preferable than arrangement (2). Let us sum the local arrangement in Figure 7b over the whole crystal: $\Sigma(^{A(m)}Na - {}^{O(3)}Y + {}^{A(2)}\square - {}^{O(3)}X) =$

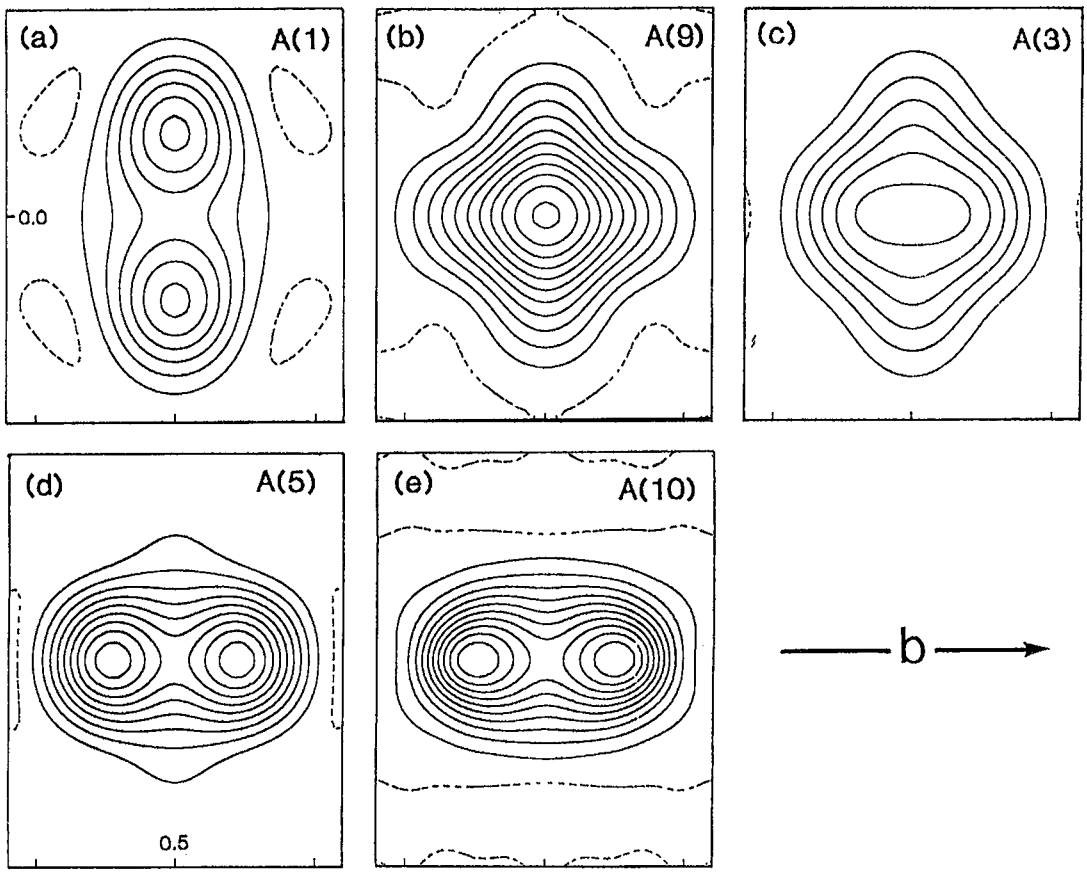


FIG. 6. Difference-Fourier maps (sections) through the *A*(2/*m*) site for crystals (a): A(1) [≡ A(2) and A(4)], (b): A(9), (c): A(3) [≡ A(7) and A(8)], (d): A(5) [≡ A(6)], and (e): A(10) [≡ A(11) and A(12)]. All maps are calculated with the *A* cations removed from the structure model and are sections parallel to $(\bar{2}01)$; the contour interval is 1 $e/Å^3$, and the broken line is the zero contour.

$^{A(m)}Na_{1.0}\,^{A(2)}\square_{1.0}\,Y_{1.0}\,X_{1.0} = {}^{A(m)}Na_1\,X_1\,Y_1$. The variation in $A(m)$ and $A(2)$ site-populations as a function of bulk composition is shown in Figure 7c. At $X = 2$ *apfu*, all $^A$Na must be associated with $X$ at O(3), and Na occupies the $A(2)$ site. As $Y$ increases, all $Y$ couples to $^A$Na and causes the $^A$Na to occur at $A(m)$. At a composition $O(3) = X_1Y_1$, all $^A$Na is coupled to $Y$ at the O(3) site, and hence all $^A$Na occurs at $A(m)$, even though O(3) is only half-occupied by $Y$. This example shows the way in which the pattern of $^A$Na ordering may change in a nonlinear fashion as a function of chemical composition, a very important point to bear in mind in the following arguments.

*The effects of K*

It now seems well established that K occurs at the $A(m)$ site. Most of the amphiboles examined here have small amounts of K in the $A$ cavity, and this must influence the form of the difference-Fourier maps obtained. However, except for A(9), all crystals have less than 0.04 K *apfu*, an amount that will have only a small influence on the difference-Fourier maps. Of most significance in this regard are crystals with maps of type (d) [A(5) and A(6)] and (e) [A(10), A(11) and A(12)]; the former crystals have no K, whereas the latter crystals have a small amount (~0.03 K *apfu*), and consequently the differences in peak shape in the difference-Fourier maps of each of these two groups of crystals cannot be due to the effects of variable K.

Crystal A(9) has considerably more K than the other crystals (0.175 K *apfu*), and this will have a significant effect on the scattering observed at the $A$ site (equivalent to ~0.32 Na *apfu*). Assuming that the K occurs at the $A(m)$ site, this suggests that the type-(b) map (Fig. 6b), which is unique to crystal A(9) in this study, is a result of the presence of significant K, and that in the absence of K, crystal A(9) would have a map of type (c).

*The effect of $^T$Al ⇌ $^T$Si and $^C$(Mg,Fe$^{2+}$) ⇌ $^C$(Al,Fe$^{3+}$) variations*

In the next section, we show that $^{O(3)}$OH ⇌ $^{O(3)}$F variation does not affect $^A$Na ordering over $A(2)$ and $A(m)$ in alkali amphiboles; thus the difference in F–OH content in fluor-nyböite (Fig. 6a: F = 1.14, OH = 0.86 *apfu*) and fluor-arfvedsonite (Fig. 8a: F = 1.62, OH = 0.38 *apfu*) is not an issue in the following argument. Fluor-nyböite (Fig. 6a) and fluor-arfvedsonite (Fig. 8a) both have $^A$Na ordered at $A(m)$. Hence the compositional difference between fluor-arfvedsonite and fluor-nyböite, namely $C = M_4^{2+}M^{3+}$ and $T = Si_8$ *versus* $C = M_3^{2+}M_2^{3+}$ and $T = Si_7Al$, does *not* result in any difference in ordering of $^A$Na in these two amphiboles.

Synthetic fluor-edenite (Boschmann *et al.* 1994) and synthetic fluor-pargasite (Oberti *et al.* 1995c; Fig. 8c) both have similar electron density at $A(2)$ and $A(m)$, although the situation is somewhat complicated, as both synthetic amphiboles have significant Ca that almost certainly occupies the $A(2)$ site. Nevertheless, the compositional difference between fluor-edenite and fluor-pargasite, $C = M_5^{2+}$ and $T = Si_7Al$ *versus* $C = M_4^{2+}Al^{3+}$ and $T = Si_6Al_2$, does not result in any difference in ordering of $^A$Na (and $^A$Ca) in these two

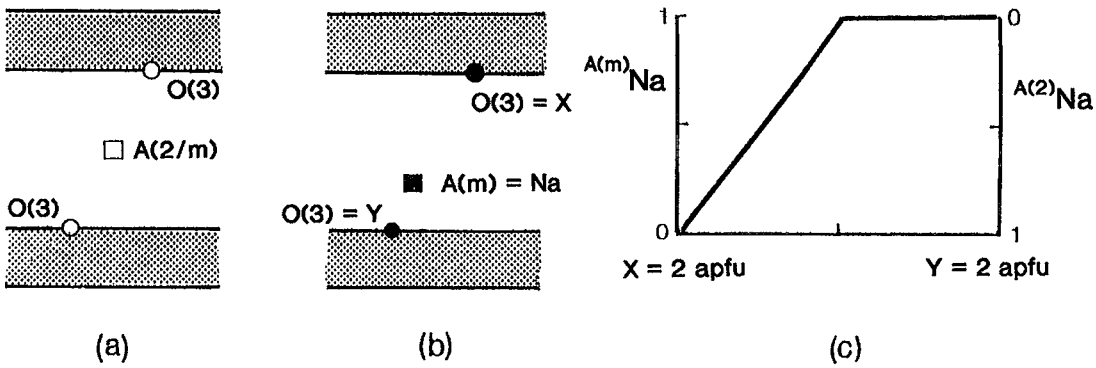


FIG. 7. Possible local ordering at the $A$ site: (a) sketch of the $A(2/m)$ site sandwiched between two octahedral strips, with the closest O(3) sites indicated; (b) occupancy of O(3) sites by anions $X^-$ and $Y^-$, with $^A$Na preferentially occupying the $A(m)$ position where locally associated with $Y^-$ rather than the $A(2)$ position where locally associated with $X^-$; (c) the resulting variation in $A(m)$ and $A(2)$ site-populations as a function of bulk anion composition of the amphibole.

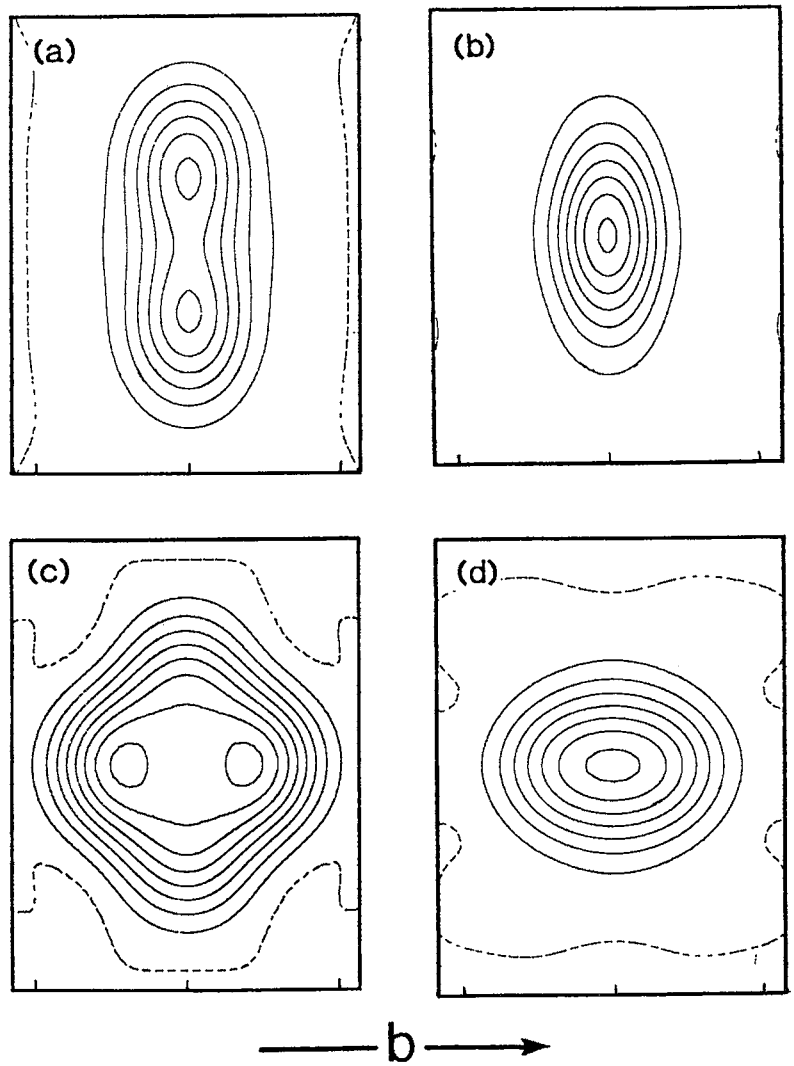


FIG. 8. Difference-Fourier map in the vicinity of the *A* site for (a) fluor-arfvedsonite [crystal A(11) of Hawthorne *et al.* 1993]; (b) arfvedsonite [crystal A(13) of Hawthorne *et al.* 1993]; (c) fluor-pargasite (Oberti *et al.* 1995c); (d) fluor-richterite (unpubl. data).

amphiboles.

Both these comparisons indicate that substitutions at the *C* and *T* sites do not necessarily correlate directly with *A*-site ordering of Na in amphiboles. This result will also be apparent in the other examples to be discussed later.

*The effect of* $^{B}Na \rightleftharpoons {}^{B}Ca$ *and* $^{O(3)}OH \rightleftharpoons {}^{O(3)}F$ *variations*

Comparison of the difference-Fourier maps for fluor-arfvedsonite (F = 1.62, OH = 0.38 *apfu*) and arfvedsonite (OH = 1.81, F = 0.19 *apfu*) (Figs. 8a, b) shows that $^{O(3)}OH \rightleftharpoons {}^{O(3)}F$ variation does not affect $^{A}Na$ ordering at *A*(*m*) where there is Na at the *M*(4) site. However, note that the displacement of the *A*(*m*) site from the center of the cavity is significantly larger for O(3) = F than for O(3) = OH. This may produce smearing of the electron density at the *A*(*m*) position in amphiboles of intermediate (OH,F) composition.

Pargasite crystals A(10), A(11) and A(12) (Figs. 6e)

have $^{A}$Na ordered at $A(2)$, whereas arfvedsonite (Fig. 8b) has $^{A}$Na ordered at $A(m)$. Both amphiboles have $C = M_4^{2+}M^{3+}$ and O(3) = OH, and hence the difference in *A*-site ordering must be due to Na *versus* Ca at $M(4)$ or Al *versus* Si at $T(1)$ (or both). However, we have shown above that Al *versus* Si does not correlate strongly with $^{A}$Na ordering. Hence, in hydroxy-amphiboles, Na at $M(4)$ causes occupancy of $A(m)$ and Ca at $M(4)$ causes occupancy of $A(2)$. We can write this in the following fashion: $^{M(4)}$Na–$^{O(3)}$OH–$^{A(m)}$Na and $^{M(4)}$Ca–$^{O(3)}$OH–$^{A(2)}$Na are preferred local configurations.

From fluor-arfvedsonite, with Na at $A(m)$ and F at O(3), we may also conclude that $^{M(4)}$Na–$^{O(3)}$F–$^{A(m)}$Na is a preferred local configuration. Now compare fluor-nyböite crystals A(1) and A(2), and nyböite crystal A(3). In crystals A(1) and A(2), there is $Na_{1.5}Ca_{0.5}$ at $M(4)$ and OH ≈ F at O(3), and only the $A(m)$ site is occupied; thus in these crystals, possible schemes of local order are $^{M(4)}$Na–$^{O(3)}$F–$^{A(m)}$Na, $^{M(4)}$Na–$^{O(3)}$OH–$^{A(m)}$Na and $^{M(4)}$Ca–$^{O(3)}$F–$^{A(m)}$Na (the *A*-site electron density in pargasite shows that $^{M(4)}$Ca–$^{O(3)}$OH–$^{A(m)}$Na does not occur). In crystal A(3), there is $Na_{1.6}Ca_{0.4}$ at $M(4)$ and OH at O(3), and the $A(2)$ and $A(m)$ sites are about equally occupied. Possible local configurations are $^{M(4)}$Na–$^{O(3)}$OH–$^{A(m)}$Na and $^{M(4)}$Ca–$^{O(3)}$OH–$^{A(2)}$Na (above, we have shown that $^{M(4)}$Na–$^{O(3)}$OH–$^{A(2)}$Na and $^{M(4)}$Ca–$^{O(3)}$OH–$^{A(m)}$Na do not occur). In crystal A(3), there is enough Ca at $M(4)$, 0.4 *apfu*, to be locally associated with Na at $A(2)$ where half the *A*-site Na occurs at $A(m)$. In crystals A(1) and A(2), $^{M(4)}$Ca–$^{O(3)}$OH–$^{A(2)}$Na cannot occur, as only $A(m)$ is occupied. From this, we may conclude that $^{M(4)}$Ca–$^{O(3)}$OH–$^{A(2)}$Na is preferred over $^{M(4)}$Na–$^{O(3)}$OH–$^{A(m)}$Na.

Consider taramite, crystals A(5) (Fig. 6d) and A(6), with $M(4) \approx Na_{0.9}Ca_{1.1}$ and $O(3) = (OH)_2$. From the last conclusion given above, we would predict that $^{M(4)}$Ca–$^{O(3)}$OH–$^{A(2)}$Na should occur (being preferred to $^{M(4)}$Na–$^{O(3)}$OH–$^{A(m)}$Na), and in accord with this prediction, taramite (Fig. 6d) has $^{A}$Na completely ordered at $A(2)$. Now consider fluor-taramite, crystal A(4) with $M(4) = Na_{1.2}Ca_{0.8}$ and $O(3) = F_1(OH)_1$; this crystal has a difference-Fourier map similar to that in Figure 6a, with Na ordered at $A(m)$, a situation dramatically different from that in taramite. Now crystal A(4) has equal amounts of OH and F at O(3). The local configuration(s) of $^{A}$Na in fluor-taramite cannot involve Ca or OH, as the $A(2)$ site is not occupied, and hence the configurations that occur are more favorable than $^{M(4)}$Ca–$^{O(3)}$OH–$^{A(2)}$Na. The possible local configurations are $^{M(4)}$Na–$^{O(3)}$F–$^{A(m)}$Na and $^{M(4)}$Ca–$^{O(3)}$F–$^{A(m)}$Na. The $^{A}$Na ordering in fluor-edenite and fluor-pargasite (Fig. 8c) indicates that $^{M(4)}$Ca–$^{O(3)}$F–$^{A(m)}$Na locally couples to $^{M(4)}$Ca–$^{O(3)}$F–$^{A(2)}$Na and does not occur as an isolated configuration. As $A(2)$ is not occupied in crystal A(4), the local configuration must be $^{M(4)}$Na–$^{O(3)}$F–$^{A(m)}$Na. Comparison of crystal A(4) with crystals A(5) and A(6) thus shows that $^{M(4)}$Na–$^{O(3)}$F–$^{A(m)}$Na is preferred over $^{M(4)}$Ca–$^{O(3)}$OH–$^{A(2)}$Na.

Consider fluor-edenite and fluor-pargasite (Fig. 8c). The $A(m)$ and $A(2)$ sites are equally occupied by Na in both crystals, indicating that the local configurations $^{M(4)}$Ca–$^{O(3)}$F–$^{A(2)}$Na and $^{M(4)}$Ca–$^{O(3)}$F–$^{A(m)}$Na occur in equal amounts. Boschmann *et al.* (1994) suggested that these two configurations are locally coupled, accounting for their occurrence in equal amounts in crystals with $M(4) = Ca_2$ and $O(3) = F_2$. Now consider crystal A(4), fluor-taramite with $M(4) = Na_{1.2}Ca_{0.8}$ and $O(3) = F_1(OH)_1$; this crystal has all $^{A}$Na ordered at $A(m)$ (Fig. 6a). Thus in A(4), configurations involving Ca, F and an occupied *A*-site must be avoided or there would be Na at $A(2)$ ($^{M(4)}$Ca–$^{O(3)}$F–$^{A(2)}$Na) owing to local coupling to $^{M(4)}$Ca–$^{O(3)}$F–$^{A(m)}$Na. As this is not the case, we can conclude that the configurations $^{M(4)}$Ca–$^{O(3)}$F–$^{A(m)}$Na and $^{M(4)}$Ca–$^{O(3)}$F–$^{A(2)}$Na are less favorable than $^{M(4)}$Na–$^{O(3)}$F–$^{A(m)}$Na.

It is difficult to evaluate the relative stability of $^{M(4)}$Ca–$^{O(3)}$F–$^{A(m)}$Na + $^{M(4)}$Ca–$^{O(3)}$F–$^{A(2)}$Na *versus* $^{M(4)}$Ca–$^{O(3)}$OH–$^{A(2)}$Na and $^{M(4)}$Na–$^{O(3)}$OH–$^{A(m)}$Na. For $^{M(4)}$Ca–$^{O(3)}$F–$^{A(m)}$Na + $^{M(4)}$Ca–$^{O(3)}$F–$^{A(2)}$Na *versus* $^{M(4)}$Ca–$^{O(3)}$OH–$^{A(2)}$Na, Nature has not been cooperative in providing the appropriate amphibole compositions. For $^{M(4)}$Ca–$^{O(3)}$F–$^{A(m)}$Na + $^{M(4)}$Ca–$^{O(3)}$F–$^{A(2)}$Na *versus* $^{M(4)}$Na–$^{O(3)}$OH–$^{A(m)}$Na, $^{M(4)}$Na–$^{O(3)}$F–$^{A(m)}$Na and $^{M(4)}$Ca–$^{O(3)}$OH–$^{A(2)}$Na would occur instead, as the resulting bulk composition would be similar. However, the fact that natural amphiboles of appropriate composition to resolve this problem do not occur (or are extremely rare and have not yet been found) suggests that the configuration $^{M(4)}$Ca–$^{O(3)}$F–$^{A(m)}$Na + $^{M(4)}$Ca–$^{O(3)}$F–$^{A(2)}$Na is less favorable than either $^{M(4)}$Ca–$^{O(3)}$OH–$^{A(2)}$Na or $^{M(4)}$Na–$^{O(3)}$OH–$^{A(m)}$Na.

## The Relative Stability of Local Configurations

We are now in a position to gather together all our conclusions in a general statement concerning the favorability of local configurations involving *A*-site ordering of Na:

$$^{M(4)}\text{Na}–^{O(3)}\text{F}–^{A(m)}\text{Na} > {}^{M(4)}\text{Ca}–^{O(3)}\text{OH}–^{A(2)}\text{Na} > {}^{M(4)}\text{Na}–^{O(3)}\text{OH}–^{A(m)}\text{Na} >> {}^{M(4)}\text{Ca}–^{O(3)}\text{F}–^{A(m)}\text{Na} = {}^{M(4)}\text{Ca}–^{O(3)}\text{F}–^{A(2)}\text{Na}$$

Again, it is important to emphasize that these are *local* configurations, and hence they may occur preferentially in amphibole structures (*i.e.*, the amphibole may show short-range order in this regard). Hence variation in *A*-site ordering will not necessarily vary linearly as a function of composition. Indeed, the pattern of *A*-site order in the sodic–calcic amphiboles examined here (Table 2) shows this to be the case.

Katophorite A(7) and A(8) both have an electron-density pattern in the *A* cavity somewhat like Figure 6c, except that the maximum density occurs in the mirror plane, rather than along the two-fold axis. The relevant site-populations for A(8) are $M(4)$ = 0.57 Na + 1.25 Ca + 0.18 $Fe^{2+}$, and O(3) = 1.65 OH + 0.35 F; from these values, we may calculate the relative occupancies of the $A(m)$ and $A(2)$ sites using the preferred local configurations listed above. The optimum configuration is $^{M(4)}Na\text{–}^{O(3)}F\text{–}^{A(m)}Na$, and the F content at O(3) allows 0.35 *apfu* of $^{A}Na$ to occur in this configuration. The next optimal configuration is $^{M(4)}Ca\text{–}^{O(3)}OH\text{–}^{A(2)}Na$, and the site occupancies allow the rest of the $^{A}Na$ (0.54 *apfu*) to occur at $A(2)$ in this configuration. Allowing for the small amount of K at $A(m)$, this gives 5.9 *epfu* (electrons per formula unit) at $A(2)$ and 4.5 *epfu* at $A(m)$, in very good agreement with the observed pattern. Katophorite A(7) behaves in a similar fashion. If the katophorite crystals A(7) and A(8) have an electron-density distribution like that shown in Figure 6c, how can nyböite, which has a significantly different chemical composition, have essentially the same electron-density distribution in the *A* cavity? The relevant site-populations for nyböite A(3) are $M(4)$ = 1.53 Na + 0.40 Ca + 0.07 $Fe^{2+}$, and O(3) = 1.77 OH + 0.23 F. The optimum configuration is $^{M(4)}Na\text{–}^{O(3)}F\text{–}^{A(m)}Na$, and the O(3) site population allows 0.23 *apfu* of the $^{A}Na$ (= F content) to occur in this configuration. The next optimum configuration is $^{M(4)}Ca\text{–}^{O(3)}OH\text{–}^{A(2)}Na$; the $M(4)$ site population allows 0.40 *apfu* of the $^{A}Na$ (= Ca content) to occur in this configuration. The remainder of the $^{A}Na$, 0.16 *apfu*, occurs as the third preferred configuration: $^{M(4)}Na\text{–}^{O(3)}OH\text{–}^{A(m)}Na$. Summing the local configurations gives the following site-populations: $A(m)$ = 0.39, $A(2)$ = 0.40 *apfu*, which agrees quite well with the observed electron-density distribution in this crystal (Fig. 6c).

Figure 8d shows the difference-Fourier map for synthetic fluor-richterite (Oberti *et al.*, unpubl. data). The arrangement of electron density is significantly different from that observed in any of the other amphiboles (Figs. 6, 8). Cameron & Gibbs (1971) and Cameron *et al.* (1983) indicated that the $A(1)$ site is occupied in this amphibole. However, we were unable to adequately represent the electron density in this amphibole by assigning Na to the $A(1)$ site with physically reasonable displacement-parameters for Na. We were also unable to adequately represent the electron density by assigning Na to the $A(2)$ and $A(m)$ sites with physically reasonable displacement-parameters for Na. A model with Na at the $A(m)$, $A(2)$ and $A(1)$ sites proved to be unstable during refinement. Hence the situation for fluor-richterite is somewhat ambiguous. What would our model predict for fluor-richterite? The $M(4)$ site is NaCa, and hence one would predict that half of the local configurations would be $^{M(4)}Na\text{–}^{O(3)}F\text{–}^{A(m)}Na$, and the remainder would be one quarter $^{M(4)}Ca\text{–}^{O(3)}F\text{–}^{A(m)}Na$ and one quarter $^{M(4)}Ca\text{–}^{O(3)}F\text{–}^{A(2)}Na$, the latter two configurations being spatially coupled. It is this latter point that may explain the unusual electron-density configuration around the *A* site in fluor-richterite. Our model proposes that $^{M(4)}Ca\text{–}^{O(3)}F\text{–}^{A(m)}Na$ and $^{M(4)}Ca\text{–}^{O(3)}F\text{–}^{A(2)}Na$ configurations are locally coupled. However, $M(4)$ is a disordered mixture of Ca and Na, and this local coupling of $^{M(4)}Ca\text{–}^{O(3)}F\text{–}^{A(m)}Na$ and $^{M(4)}Ca\text{–}^{O(3)}F\text{–}^{A(2)}Na$ may be frustrated by the occurrence of Ca and Na rather than Ca and Ca at adjacent $M(4)$ sites. Thus an unusual and very disordered cation arrangement occurs in the *A* cavity in end-member synthetic fluor-richterite.

## The Crystal-Chemical Basis for Ordering Behavior

### *The effect of F versus OH at O(3)*

It is apparent from the above analysis of electron-density patterns that the constitution of the O(3) site has a significant effect on the ordering of Na at the *A* site. In alkali amphiboles, $^{A}Na$ orders at $A(m)$ whether O(3) is occupied by F or by OH. However, the electron density at the *A* site in fluor-arfvedsonite (Fig. 8a) shows two well-defined maxima, whereas the corresponding electron-density in arfvedsonite (Fig. 8b) shows only one central maximum with elongation within the mirror plane. Thus the occupancy of O(3) significantly affects the coordinates of the $A(m)$ site (although there will also be a difference due to the *A* site containing significant K in the arfvedsonite of Fig. 8b). The reason for this is the potential interaction of $^{A(m)}Na$ with H in arfvedsonite. We inserted a H atom at the appropriate position in *fluor-arfvedsonite,* and the resulting $A(m)$–H distance was 2.35 Å, which is much too short for a stable Na–H approach that does not involve a hydride bond. Thus in arfvedsonite, in which the O(3) site is occupied by OH, Na at the $A(m)$ site must avoid the H atom bonded to O(3), with the result that the $A(m)$–$A(m)$ separation in arfvedsonite (Fig. 8b) is much smaller than it is in fluor-arfvedsonite.

A similar effect occurs in calcic amphiboles. In fluor-edenite (Boschmann *et al.* 1994) and fluor-pargasite (Oberti *et al.* 1995c), $^{A}Na$ is equally partitioned between the $A(m)$ and $A(2)$ sites, whereas in pargasite (Fig. 6e), $^{A}Na$ is ordered at the $A(2)$ site. Insertion of a H atom into the fluor-edenite structure would place it only 2.39 Å from the $A(m)$ site, and hence $^{A}Na$ cannot occupy *this* $A(m)$ site [*i.e.*, adjacent to an OH at the O(3) site]. Why doesn't the $^{A}Na$ occupy an $A(m)$ site with a smaller displacement from the central $A(2/m)$ site in pargasite? Presumably, this question relates to the more general question of bond-valence requirements; it will be discussed in the next section.

*Bond-valence considerations*

The *A* cation must order within the *A* cavity such that all local bond-valence requirements are satisfied, and this is the underlying reason why the pattern of order of the *A* cation is dictated by the preferential occurrence of local (short-range) arrangements rather than being a linear function of crystal composition. This being the case, it seems anomalous, at first sight, that differences in $^{[4]}$Al content do not induce differences in ordering behavior [*cf.* fluor-nyböite (Fig. 6a) and fluor-arfvedsonite (Fig. 8a), and synthetic fluor-edenite (Boschmann *et al.* 1994) and synthetic fluor-pargasite (Oberti *et al.* 1995c)], as the bond valence incident at O(5), O(6) and O(7) is strongly affected by the presence of Al or Si at the adjacent *T* sites.

It is necessary to realize that *all* calcic amphiboles with a full *A*-site have at least 1.0 $^{[4]}$Al, and hence the effects of $^{[4]}$Al *tend* to be associated with the effects of $^{M(4)}$Ca. Of course, this is not entirely the case, as nyböite is an alkali amphibole and yet has $^{[4]}$Al. However, later we shall show that the alkali amphiboles respond differently from the calcic amphiboles to the incorporation of $^{[4]}$Al, and so the effects of $^{[4]}$Al tend to be parallel to the effects of Ca or Na in each structure type.

Table 9 shows the Pauling bond-strengths and bond-valences [calculated from the curves of Brown (1981)] around the O(5), O(6) and O(7) atoms in selected amphibole structures. It is immediately apparent from the Pauling bond-strength sums that the O(5) and O(6) anions receive an excess of incident bond-strength from the *T* and *M*(4) cations and, as indicated by the analogous bond-valences, the structure adapts to reduce the incident bond-valence at these anions. The situation at O(7) is somewhat different. In $^{[4]}$Al-bearing amphiboles, there is a deficiency of incident bond-strength, and the incident bond-valence sums decrease with increasing $^{[4]}$Al (Table 9), whereas in $^{[4]}$Al-free amphiboles, there is not a deficiency in incident bond-strength at O(7), but the incident bond-valence sum is significantly less that the ideal value of 2 valence units (*vu*). It is thus apparent from the range of bond-strength and bond-valence sums in Table 9 that incorporation of an alkali cation into the *A* cavity must involve a significant bond-valence contribution to the O(7) anion while avoiding an excessive contribution to the O(5) and O(6) anions. It is also apparent from Table 9 that the valence-sum rule of Brown (1981) cannot hold at the O(5), O(6) and O(7) anions. There are twelve anions surrounding the *A* cavity, and ten can be considered as potentially bonding to an *A* cation at the *A*(*m*) or *A*(2) sites. The total ideal bond-strength and bond-valence required by these ten anions [4 × O(5) + 4 × O(6) + 2 × O(7)] is 4 × 2 + 4 × 2 + 2 × 2 = 20 *vu*. The bond-strength and bond-valence contributions required from the *A* cation by these ten anions can be calculated from the bond-strength and bond-valence sums listed in Table 10. For arfvedsonite (Table 10), the bond-strength and bond-valence contributions, $\Delta_{bs}$ and $\Delta_{bv}$, are given by $\Delta_{bs} = 20 - 4 \times 2.13 - 4 \times 2.13 - 2 \times 2.00 = -1.04$ and $\Delta_{bv} = 20 - 4 \times 1.953 - 4 \times 2.105 - 2 \times 1.928 = -0.088$ *vu*, respectively. According to Table 9, the total bond-valence, $\Delta$, required by the anions surrounding the *A* site [4 × O(5) + 4 × O(6) + 2 × O(7)] is approximately zero for arfvedsonite and nyböite, and only becomes the ideal value of 1.0 *vu* in sadanagaite. Essentially, we can think of the *A* cavity as becoming much more basic from $^{[4]}$Al-free alkali amphiboles to $^{[4]}$Al-bearing calcic amphiboles, and requiring a stronger Lewis acid in the *A* cavity. Thus in amphiboles with low basicity of the *A* cavity, the *A* cation will seek to minimize its Lewis acidity by maximizing its coordination number; in alkali amphiboles, $^{A}$Na thus occupies the *A*(*m*) site with an effective coordination number of [9]. In amphiboles with high basicity of the *A* cavity, the *A* cation will seek to maximize its Lewis acidity by minimizing its coordination number, that is by occupying the *A*(2) site with an effective coordination number of [6]. This argument is in accord with the bond valence to the *A* cations in arfvedsonite and pargasite (Table 10). The alkali amphiboles arfvedsonite and nyböite have $\Delta \approx 0$ *vu* [and *A*(*m*) = Na], and the calcic amphiboles pargasite and sadanagaite have $\Delta \approx 0.8$–1.0 *vu* [and *A*(2) = Na]; fluor-edenite and fluor-pargasite have $\Delta \approx 0.25$ and 0.68 *vu*, respectively, and Na splits between the *A*(*m*) and *A*(2) sites, in accord with their intermediate $\Delta$ values.

## The Chemical Composition of Natural Amphiboles

Locally favorable configurations will exert an influence on the chemical composition of amphiboles, as combinations of components that form favorable local configurations will be preferentially incorporated into the growing crystal. From the general statement of relative preference of local configurations, we can conclude that, in natural systems in which both OH and F are readily available, alkali amphiboles should tend to be F-rich [up to a composition $(OH)_1F_1$], whereas calcic amphiboles will be F-poor. Furthermore, the variations in F in calcic amphiboles should tend to show a positive (but not necessarily linear) correlation with the Na content at *M*(4). These compositions tend to occur in igneous parageneses where evolving fractionation involves calcic → sodic amphibole evolution, together with F enrichment in the later stages. These very general correlations support our major conclusion on the relative stability of local configurations. Furthermore, the relative stability of these local configurations provides a mechanism for controlling the general compositional trends involving the *A*- and *B*-group cations and the monovalent anions.

TABLE 9. BOND STRENGTHS (bs) AND BOND VALENCE (bv in *vu*) INCIDENT AT THE O(5), O(6) AND O(7) ANIONS IN SELECTED AMPHIBOLES*

| | Arfvedsonite | | Nybøite | | Fluor-edenite | | Pargasite | | Sadanagaite | |
|---|---|---|---|---|---|---|---|---|---|---|
| | bs | bv | bs | bv | bs | bv | bs | bv | bs | bv |
| O(5)–*T*(1) | 1.00 | 0.982 | 0.94 | 0.944 | 0.94 | 0.876 | 0.88 | 0.845 | 0.88 | 0.843 |
| O(5)–*T*(2) | 1.00 | 1.894 | 1.00 | 0.951 | 1.00 | 0.927 | 1.00 | 0.944 | 0.95 | 0.903 |
| O(5)–*M*(4) | 0.13 | 0.077 | 0.13 | 0.102 | 0.25 | 0.173 | 0.25 | 0.187 | 0.25 | 0.188 |
| Σ | 2.13 | 1.953 | 2.07 | 1.997 | 2.19 | 1.976 | 2.13 | 1.976 | 2.08 | 1.934 |
| O(6)–*T*(1) | 1.00 | 0.987 | 0.94 | 0.941 | 0.94 | 0.882 | 0.88 | 0.847 | 0.88 | 0.834 |
| O(6)–*T*(2) | 1.00 | 0.982 | 1.00 | 0.917 | 1.00 | 0.892 | 1.00 | 0.901 | 0.95 | 0.887 |
| O(6)–*M*(4) | 0.13 | 0.136 | 0.13 | 0.158 | 0.25 | 0.280 | 0.25 | 0.192 | 0.25 | 0.209 |
| Σ | 2.13 | 2.105 | 2.07 | 2.016 | 2.19 | 2.054 | 2.13 | 1.940 | 2.08 | 1.930 |
| O(7)–*T*(1) x2 | 2.00 | 1.928 | 1.87 | 1.886 | 1.87 | 1.816 | 1.75 | 1.760 | 1.75 | 1.769 |
| $\Delta_{bs}$ ** | −1.04 | | 0.86 | | −1.26 | | −0.54 | | −0.14 | |
| $\Delta_{bv}$ ** | −0.088 | | −0.062 | | 0.248 | | 0.816 | | 1.006 | |

Arfvedsonite $(K_{0.59}Na_{0.36})(Na_{1.63}Ca_{0.07})(Fe^{2+}_{3.26}Mn^{2+}_{0.16}Fe^{3+}_{1.33}Li_{0.15}Ti^{4+}_{0.06})(Si_{7.89}Al_{0.14})O_{22}(OH)_{1.81}F_{0.19}$

Nybøite $(K_{0.04}Na_{0.76})(Na_{1.53}Ca_{0.40}Fe^{2+}_{0.07})(Mg_{2.77}Fe^{2+}_{0.90}Fe^{3+}_{0.39}Al_{1.36}Ti^{4+}_{0.03})(Si_{6.91}Al_{1.09})O_{22}(OH)_{1.77}F_{0.23}$

Fluor-edenite $(Na_{0.92}Ca_{0.09})(Ca_{1.85}Mg_{0.15})(Mg_{4.64}Al_{0.36})(Si_{6.56}Al_{1.44})O_{22}F_2$

Pargasite $(K_{0.04}Na_{0.96})(Ca_{1.76}Na_{0.24}Mn^{2+}_{0.01})(Mg_{3.23}Fe^{2+}_{0.65}Fe^{3+}_{0.03}Al_{1.07})(Si_{6.12}Al_{1.88})O_{22}(OH)_{1.97}F_{0.03}$

Sadanagaite $(K_{0.30}Na_{0.83})(Ca_{1.74}Na_{0.12}Fe^{2+}_{0.14})(Mg_{1.17}Fe^{*}_{.07}Fe^{3+}_{0.78}Ti^{4+}_{0.39}Al_{0.69})(Si_{5.27}Al_{2.73})O_{22}(OH)_2$

* Nybøite: A(3), this study; arfvedsonite: A(13), Hawthorne *et al.* (1993); fluor-edenite: Boschmann *et al.* (1994); pargasite: A(12), this study; sadanagaite: refined by Hawthorne & Grundy (1977) under the pseudonym of subsilicic titanian magnesian hastingsite.

** Total bond-strength and bond-valence required by 4 x O(5) + 4 x O(6) + 2 x O(7) anions to agree with the valence-sum rule exactly (averaged over the anions).

## CONCLUSIONS

1. The pattern of electron-density distribution in the *A* cavity of Na-bearing K-free *C2/m* amphiboles is highly variable. There may be one or two or four maxima in the electron density, all maxima occurring at the *A*(*m*), *A*(2) or *A*(2/*m*) positions.
2. The observed electron-density patterns and their variations as a function of site populations in the amphibole structure can be interpreted in terms of a series of short-range configurations involving atoms at the *M*(4), O(3) and *A* sites.
3. The relative preference of these short-range ordering patterns is $^{M(4)}Na\text{–}^{O(3)}F\text{–}^{A(m)}Na > {}^{M(4)}Ca\text{–}{}^{O(3)}OH\text{–}^{A(2)}Na > {}^{M(4)}Na\text{–}{}^{O(3)}OH\text{–}^{A(m)}Na >> {}^{M(4)}Ca\text{–}{}^{O(3)}F\text{–}^{A(m)}Na = {}^{M(4)}Ca\text{–}{}^{O(3)}F\text{–}^{A(2)}Na$.
4. The conformation of these patterns of short-range order may be rationalized on the basis of local bond-valence requirements.

TABLE 10. BOND VALENCES (*vu*) AROUND THE *A*(*m*) AND *A*(2) SITES IN ARFVEDSONITE AND PARGASITE

| Arfvedsonite | | Pargasite | |
|---|---|---|---|
| *A*(*m*)–O(5) x2 | 0.066 | *A*(2)–O(5) x2 | 0.124 |
| *A*(*m*)–O(5) x2 | 0.088 | *A*(2)–O(6) x2 | 0.111 |
| *A*(*m*)–O(6) x2 | 0.115 | *A*(2)–O(7) x2 | 0.167 |
| *A*(*m*)–O(7) | 0.162 | Σ | 0.804 |
| *A*(*m*)–O(7) | 0.130 | | |
| *A*(*m*)–O(7) | 0.065 | <bv> | 0.134 |
| Σ | 0.895 | | |
| <bv> | 0.099 | | |

## ACKNOWLEDGEMENTS

We thank Mike Phillips, an anonymous reviewer, Associate Editor Roland Rouse and even Editor Bob Martin for their comments that materially improved the clarity of this paper. FCH acknowledges the support of a Killam Fellowship and an Operating Grant from the Natural Sciences and Engineering Research Council of Canada.

## REFERENCES

BOCCHIO, R., UNGARETTI, L. & ROSSI, G. (1978): Crystal chemical study of eclogitic amphiboles from Alpe Arami, Lepontine Alps, southern Switzerland. *Soc. Ital. Mineral. Petrol. Rend.* **24**, 453-470.

BOSCHMANN, K.F., BURNS, P.C., HAWTHORNE, F.C., RAUDSEPP, M. & TURNOCK, A.C. (1994): A-site disorder in synthetic fluor-edenite, a crystal structure study. *Can. Mineral.* **32**, 21-30.

BROWN, I.D. (1981): The bond-valence method: an empirical approach to chemical structure and bonding. *In* Structure and Bonding in Crystals II (M. O'Keeffe & A. Navrotsky, eds.). Academic Press, New York (1-30).

CAMERON, M. & GIBBS, G.V. (1971): Refinement of the crystal structure of two synthetic fluor-richterites. *Carnegie Inst. Wash., Year Book* **70**, 150-153.

_____, SUENO, S., PAPIKE, J.J. & PREWITT, C.T. (1983): High temperature crystal-chemistry of K and Na fluor-richterites. *Am. Mineral.* **68**, 924-943.

GIBBS, G.V. (1966) Untitled article. *In* AGI Short Course Lecture Notes on Chain Silicates, 1-23.

_____ & PREWITT, C.T. (1968): Amphibole cation site disorder. *In* Int. Mineral. Assoc., Pap. Proc. Fifth Gen. Meet. (Cambridge, 1966). Mineralogical Society, London, U.K. (abstr.).

HAWTHORNE, F.C. (1983): The crystal chemistry of the amphiboles. *Can. Mineral.* **21**, 173-480.

_____ & GRUNDY, H.D. (1972): Positional disorder in the A-site of clino-amphiboles. *Nature (Phys. Sci.)* **235**, 72-73.

_____ & _____ (1973a): The crystal chemistry of the amphiboles. I. Refinement of the crystal structure of ferrotschermakite. *Mineral. Mag.* **39**, 36-48.

_____ & _____ (1973b): The crystal chemistry of the amphiboles. II. Refinement of the crystal structure of oxy-kaersutite. *Mineral. Mag.* **39**, 390-400.

_____ & _____ (1978): The crystal chemistry of the amphiboles. VII. The crystal structure and site chemistry of potassian ferri-taramite. *Can. Mineral.* **16**, 53-62.

_____, GRIEP, J.L. & CURTIS, L. (1980): A three-amphibole assemblage from the Tallan Lake sill, Peterborough County, Ontario. *Can. Mineral.* **18**, 275-284.

_____, UNGARETTI, L., OBERTI, R., BOTTAZZI, P. & CZAMANSKE, G.K. (1993): Li: an important component in igneous alkali amphiboles. *Am. Mineral.* **78**, 733-745.

HERITSCH, H. (1955): Bemerkungen zur Schreibung der kristallchemischen Formel der Hornblende. *Tschermaks Mineral. Petrogr. Mitt.* **5**, 242-245.

OBERTI, R., HAWTHORNE, F.C., UNGARETTI, L. & CANNILLO, E. (1995b): $^{[6]}$Al disorder in amphiboles from mantle peridotites. *Can. Mineral.* **33**, 867-878.

_____, SARDONE, N., HAWTHORNE, F.C., RAUDSEPP, M. & TURNOCK, A.C. (1995c): Synthesis and crystal-structure refinement of synthetic fluor-pargasite. *Can. Mineral.* **33**, 25-31.

_____, UNGARETTI, L., CANNILLO, E. & HAWTHORNE, F.C. (1992): The behaviour of Ti in amphiboles. I. Four- and six-coordinated Ti in richterite. *Eur. J. Mineral.* **4**, 425-439.

_____, _____, _____, _____ & MEMMI, I. (1995a): Temperature-dependent Al order–disorder in the tetrahedral double-chain of *C2/m* amphiboles. *Eur. J. Mineral.* **7**, 1049-1063.

PAPIKE, J.J., ROSS, M. & CLARK, J.R. (1969): Crystal-chemical characterization of clinoamphiboles based on five new structure refinements. *Mineral. Soc. Am., Spec. Pap.* **2**, 117-136.

PREWITT, C.T. (1963): Crystal structures of two synthetic amphiboles. *Geol Soc. Am., Spec. Pap.* **76**, 132-133 (abstr.).

UNGARETTI, L. (1980): Recent developments in X-ray single crystal diffractometry applied to the crystal-chemical study of amphiboles. *God. Jugoslav. Kristalogr.* **15**, 29-65.

_____, SMITH, D.C. & ROSSI, G. (1981): Crystal-chemistry by X-ray structure refinement and electron microprobe analysis of a series of sodic–calcic to alkali-amphiboles from the Nybö eclogite pod, Norway. *Bull. Minéral.* **104**, 400-412.

*Received July 8, 1995, revised manuscript accepted January 6, 1996.*